UCLA

Data Assimilation, and Forecasting the near-Earth Radiation Environment

Adam C. Kellerman[1], Y. Y. Shprits[1,3], T. Podladchikova[4], A. Drozdov[1], H. Zhu[5], D. Kondrashov[2]

1. Department of Earth, Planetary, and Space Sciences, UCLA
2. Department of Atmospheric and Ocean Sciences, UCLA
3. GFZ German Research Centre for Geosciences, University of Potsdam, Germany
4. Skolkovo Institute of Technology, Skolkovo, Russia
5. University of Texas, Dallas

Presentation Outline

1. VERB
2. GOES/Van Allen Probe data
3. Data Assimilation
4. Data Assimilative Forecasting with VERB
5. A long-term reanalysis dataset

Versatile Electron Radiation Belt code

The VERB code models the global state and evolution of the Earth's radiation belt electrons

What's special about this code?

1. We operate in an invariant coordinate system, where radiation particles 'live'
2. The code is fast, and can be run on a personal computer due to its advanced, and accurate, numerical architecture

Observations (data)

GOES 13 and 15:

MagED and EPEAD: 10’s of keV to ~2 MeV

Van Allen Probe A & B:

MagEIS: 10’s of keV to MeV

Coverage at GEO and through GTO

Solar Wind/Geomagnetic Indices

SWPC: 3-day forecast Kp index:

:Product: 3-Day Forecast
:Issued: 2017 Sep 08 0045 UTC
Prepared by the U.S. Dept. of Commerce, NOAA, Space Weather Prediction Center
#
A. NOAA Geomagnetic Activity Observation and Forecast

The greatest observed 3 hr Kp over the past 24 hours was 8 (NOAA Scale G4).
The greatest expected 3 hr Kp for Sep 08-Sep 10 2017 is 8 (NOAA Scale G4).

NOAA Kp index breakdown Sep 08-Sep 10 2017

	Sep 08	Sep 09	Sep 10
00-03UT	8 (G4)	7 (G3)	5 (G1)
03-06UT	6 (G2)	6 (G2)	4
06-09UT	5 (G1)	5 (G1)	4
09-12UT	4	4	4
12-15UT	4	4	4
15-18UT	6 (G2)	4	4
18-21UT	6 (G2)	4	4
21-00UT	7 (G3)	4	4

Rationale: G1-G4 (Minor-Sever) geomagnetic storm levels are expected on day one (08 Sep) and G1-G3 (Minor-Strong) storm levels on day two due to the combined influence of the 04 Sep and 06 Sep CMEs.

SWPC: Ace data:

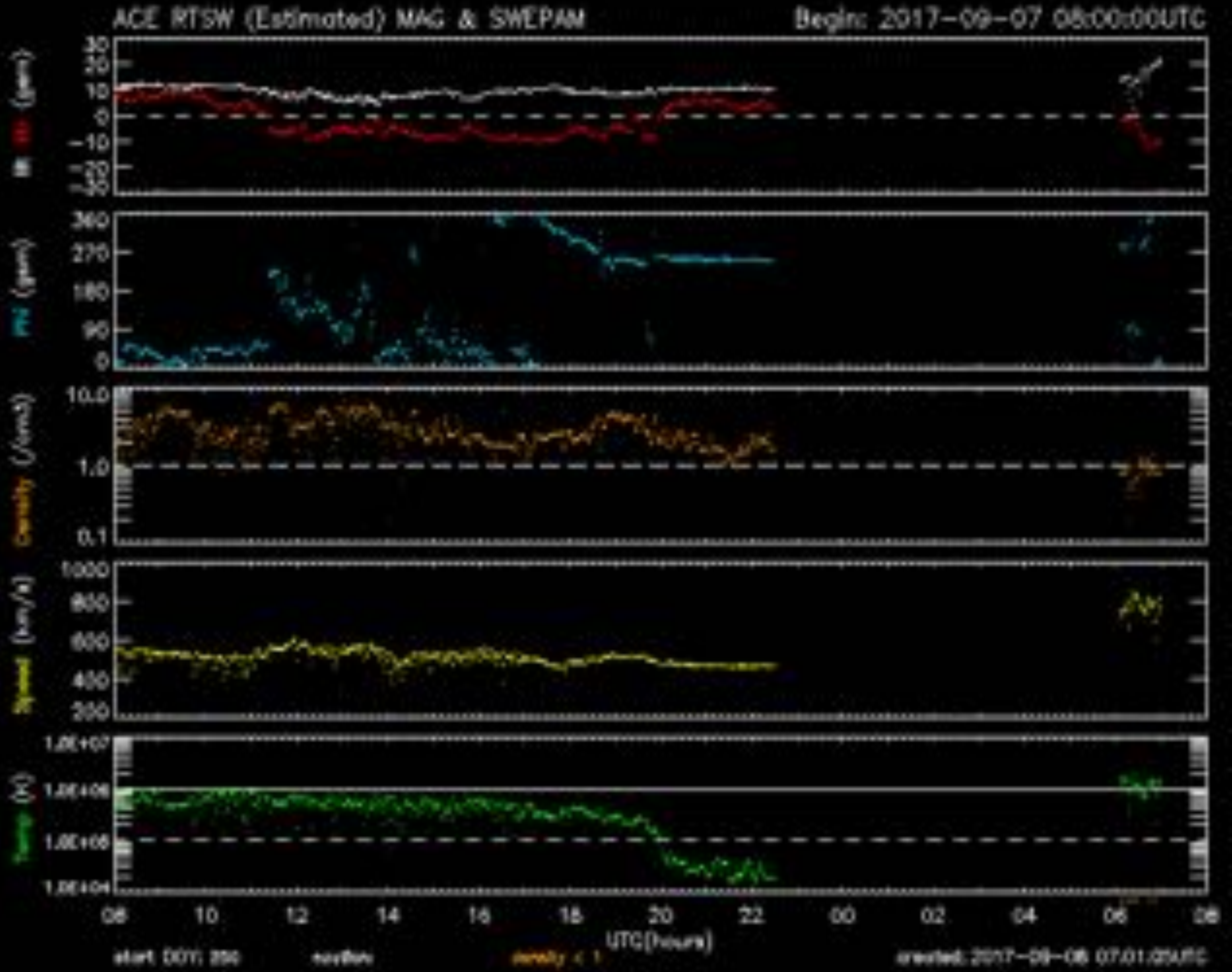

Data Assimilation

Individually, data and models may not accurately specify the environment

Model

Global estimate with
some error and bias

Data

Sparse observation with
some error and bias

Data Assimilation

If we combine the model and data, we may obtain an estimate closer to the truth

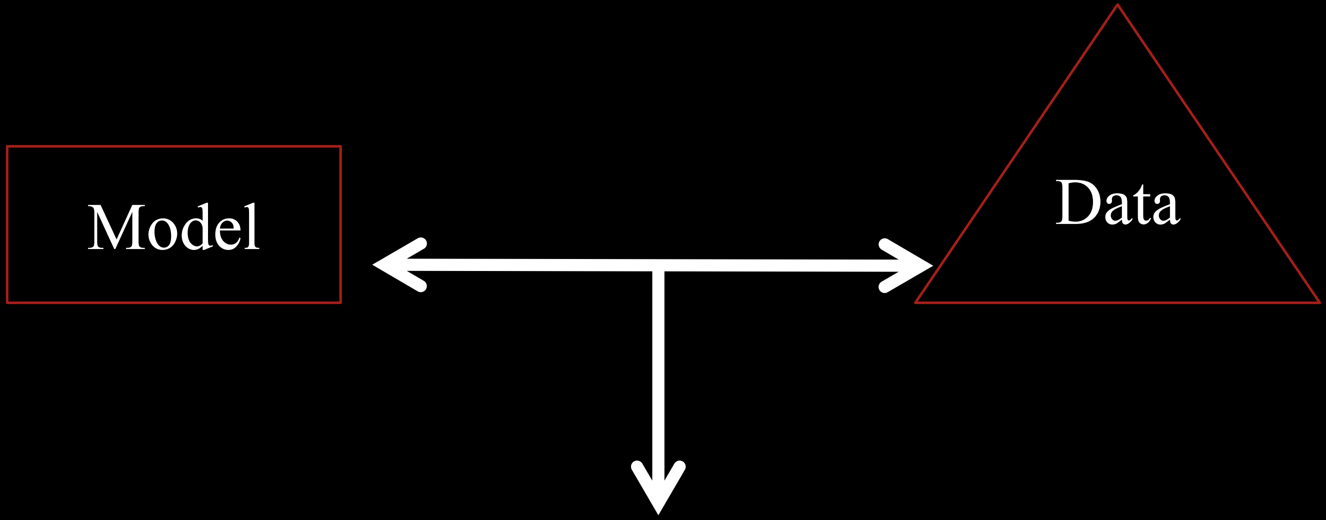

Global coverage with a smaller overall error and bias

Radiation Belt Forecast Framework

UCLA

Real-time Van Allen Probe data

Real time GOES 13 and 15 data

Real time and forecast Kp (SWPC)

Real time ACE solar wind (SWPC)

```
# Radiation Belt Forecast Cron Script
# Written by A. C. Kellerman

3 */2 * * * . /home/akellerman/.bashrc; /home/akellerman/projects/RBSP_realtime/branches/UCLA/codes/run_sw_prop.sh #load and propagate solar wind data
4 */2 * * * . /home/akellerman/.bashrc; /home/akellerman/projects/GOES/code/realtime_goes_main.sh #process goes realtime, including L*
18 */2 * * * . /home/akellerman/.bashrc; /home/akellerman/data/Kp/Kp_3day/run_proc_kp.sh #SWPC kp
20 */2 * * * . /home/akellerman/.bashrc; /home/akellerman/projects/GREEP_code/branches/kp_den_vsw_lvl/matlab/run_greep_forecast.sh #GREEP forecast with added sophisication
25 */2 * * * . /home/akellerman/.bashrc; /home/akellerman/projects/GREEP_code/branches/invariant_greep/matlab/run_greep_forecast.sh #GREEP forecast with invariants and PSD
31 */2 * * * /home/akellerman/rsync_rb_realtime.sh # rsync rb realtime folders
32 */2 * * * . /home/akellerman/.bashrc; /home/akellerman/projects/RBSP_realtime/branches/UCLA/codes/run_proc_rb.sh #realtime rb
59 */2 * * * . /home/akellerman/.bashrc; /home/akellerman/projects/VERB_code_2.0/Real_time/run_DA_forecast_Neumann.sh # run forecast version 2
30 4 * * * . /home/akellerman/.bashrc; /home/akellerman/data/Kp/Kp_archive/run_process_kp.sh #process final kp
0 4 * * * . /home/akellerman/.bashrc; /home/akellerman/gitlab_backups/run_gitlab_backup.sh
```

Data Assimilation

Forecast radiation belt state

Nowcast radiation belt state

Data
Model
Process
Product

Global Radiation Belt Forecast

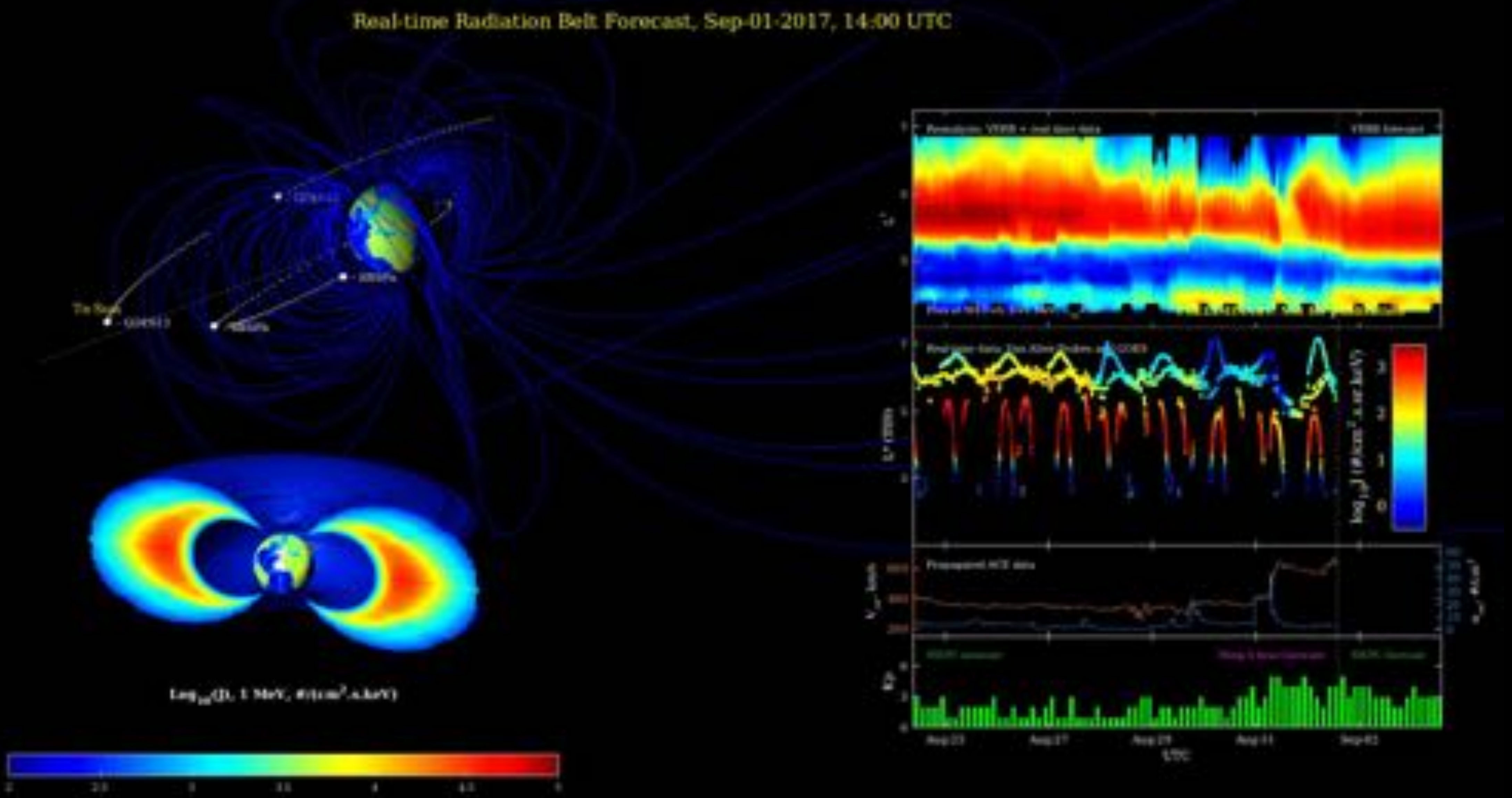

Robust During Data Outage

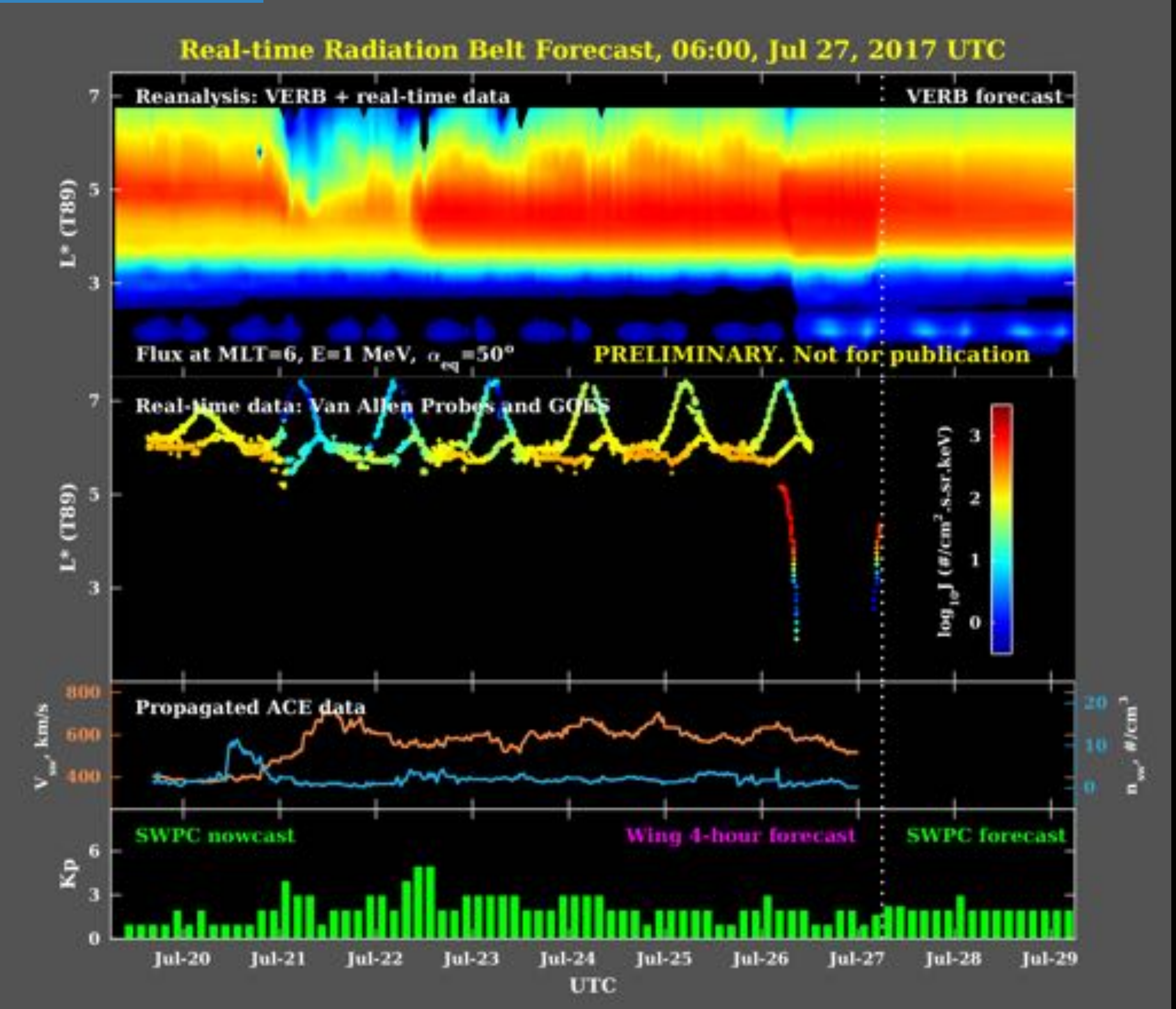

Data assimilation allows to account for hysteresis (bias) effects

Data are sparse, often missing, or have processing errors. There are many gaps

Reanalysis allows for reconstruction of the radiation belt fluxes, even when data are missing

Here we highlight the importance of GOES data for our forecast framework

Forecast solar wind data are limited

In order to test and validate model performance, a study of forecast performance using final data is required

http://rbm.epss.ucla.edu/realtime-forecast/

A Long-Term Global Dataset

We have a 4-year dataset of radiation belt-electron reanalysis
currently 2012-2016
Will be extended back to 1995

Such a dataset can be useful for specifying the environment around a given spacecraft

Averaging over time, energy, and space can be accomplished for 100 keV to multi-MeV electrons

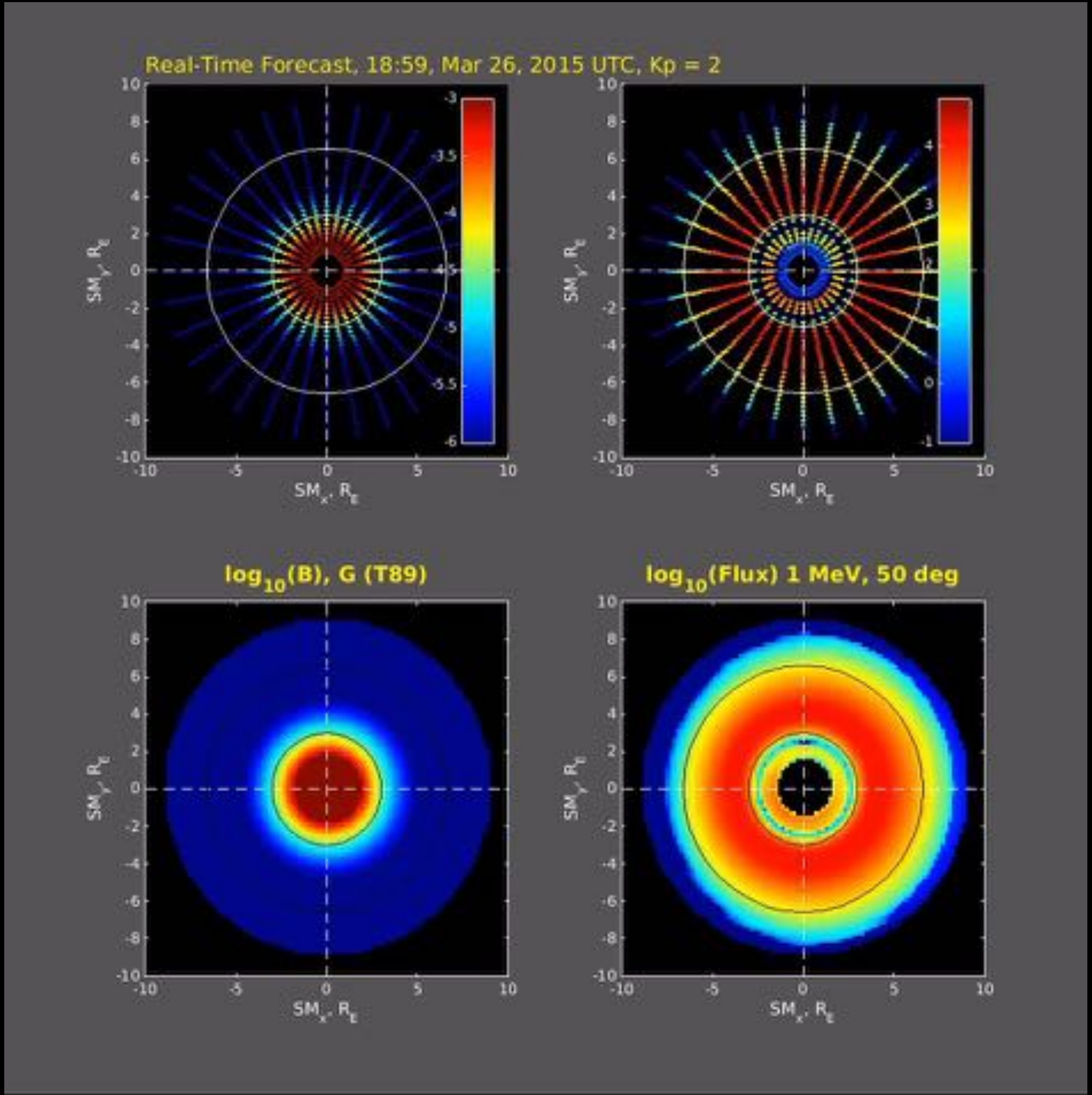

Summary

1. Implemented a robust and fast data-assimilation method for VERB 2.0

2. Real-time radiation belt nowcasts and forecasts using data assimilation - running every 2 hours, begun in 2015 – SWPC & APL

3. A long-term dataset of globally reconstructed fluxes is available from 2012-2016. This will be extended back to 1995, and forward as more data are available

4. Forecast validation has been complete – a more accurate and advanced model will be released in the near future

Space Weather Effects

Radiation is hazardous to satellite electronics & humans in space

Over 3,000 satellites; Supporting $25B/yr industry; Replacement cost: over $75B; GPS industry ~ $1 trillion

Electric-orbit raising ~6 month transition through the belts

Space radiation impacts polar flights (~7,000) (cost ~$0.1 M per flight) examples: NY -Tokyo; LA - Moscow; disruption of power grids, produces blackouts (up to $100M in losses)

A Carrington type storm (1859) may cause $0.6-2.6 trillion in damage

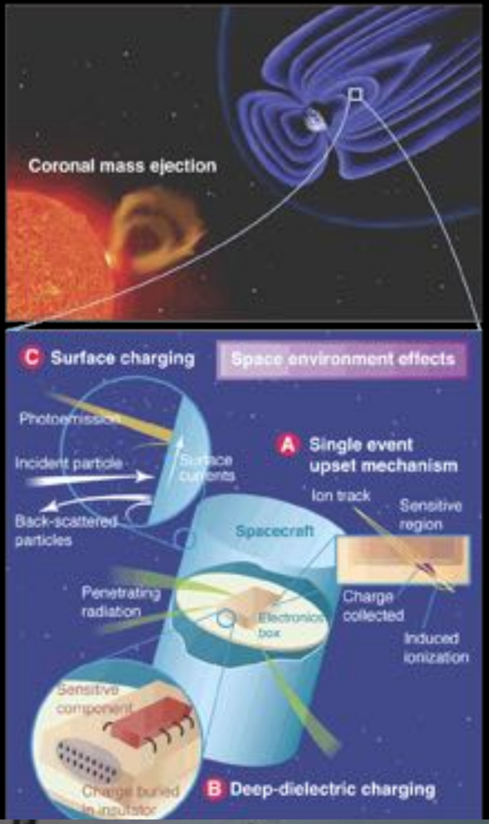




Particle Motion

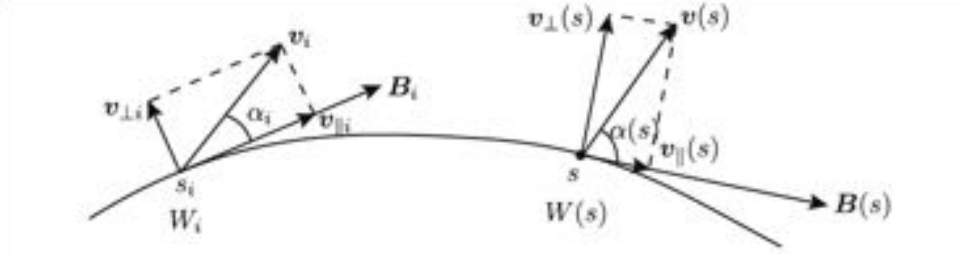

Fig. 2.6 Change of $v_\perp$ and $v_\parallel$ vectors along a magnetic field line

$$\tau_b = 2\int_{s'_m}^{s_m} \frac{ds}{v_\parallel(s)} = \frac{2}{v}\int_{s'_m}^{s_m} \frac{ds}{[1 - B(s)/B_m]^{\frac{1}{2}}} \qquad (2.34)$$

Bounce period for a particle on an equipotential field line. The integrable singularity at the mirror points poses a problem.

We can use a change of variables

$$1 - B/B_m = \cos^2 \alpha_{eq} \sin^2 \psi,$$

Orlova and Shprits, [2011]

$$ds = (ds / dB)dB = (ds / dB)(dB / d\psi)d\psi$$

$$\tau_B = -4/v \cos \alpha_{eq} B_m \int_0^\pi ds/ dB \cos \psi d\psi.$$

$$\lim_{\psi \to \pi/2} \frac{\cos\psi}{dB / ds} = -\lim_{\psi \to \pi/2} \frac{\sin\psi}{d^2 B / ds^2}\frac{d\psi}{ds} = -\frac{\tan^2 \alpha_{eq}}{2B_{eq}}\left(\frac{ds}{d\psi}\right)_{eq}$$

In this way, we can compute the bounce time using standard numerical approaches at all points along the bounce orbit

$$J = \oint p_\parallel ds = m \oint v\, \mu\, ds$$

$$K = \frac{J}{2\sqrt{2mM}} = I\sqrt{B_m}$$

$$I = \int_{s'_m}^{s_m} [1 - B(s)/B_m]^{\frac{1}{2}} ds$$

We use MPI-FORTRAN routines to trace particles at high precision in a realistic time-dependent magnetic field model, and compute I, τ, and the δI/δr

Particle Motion

$$\langle V_0 \rangle = \frac{\nabla_0 J \times e_0}{q \tau_b B_0}$$

How do we compute the bounce-averaged gradient and curvature drift velocity?

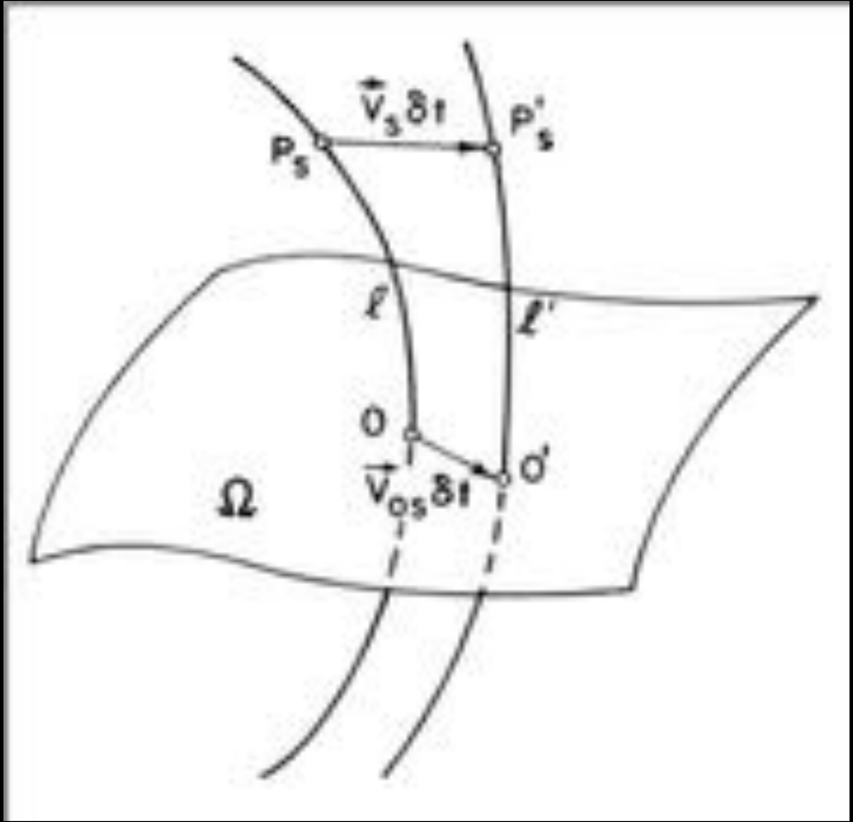

$$I = \int_{s'_m}^{s_m} [1 - B(s)/B_m]^{\frac{1}{2}} ds$$

Related to the second invariant J = 2pI

We compute I numerically in a realistic magnetic field model, in order to match our predetermined grid in K.

We obtain I for the reference field line, as well as Bm, alpha, and the gradient of I.

The location of the mirror point allows us to compute a time-dependent and MLT-dependent loss cone.

Last, we also compute the E x B drift using a Volland-Stern E-field.

The Radiation Belts

Adiabatic invariants are conserved for electron energies of 100’s of keV to several MeV, which form the electron radiation belts.

Electron radiation belts typically consist of an inner and an outer belt

‘Slot’ region caused by scattering of particles, principally plasmaspheric hiss [*Lyons and Thorne*, 1973; *Abel and Thorne*, 1998]

The inner region is very stable and particles have a very long lifetime ~ years

The outer region is much more dynamic and is a topic of ongoing study

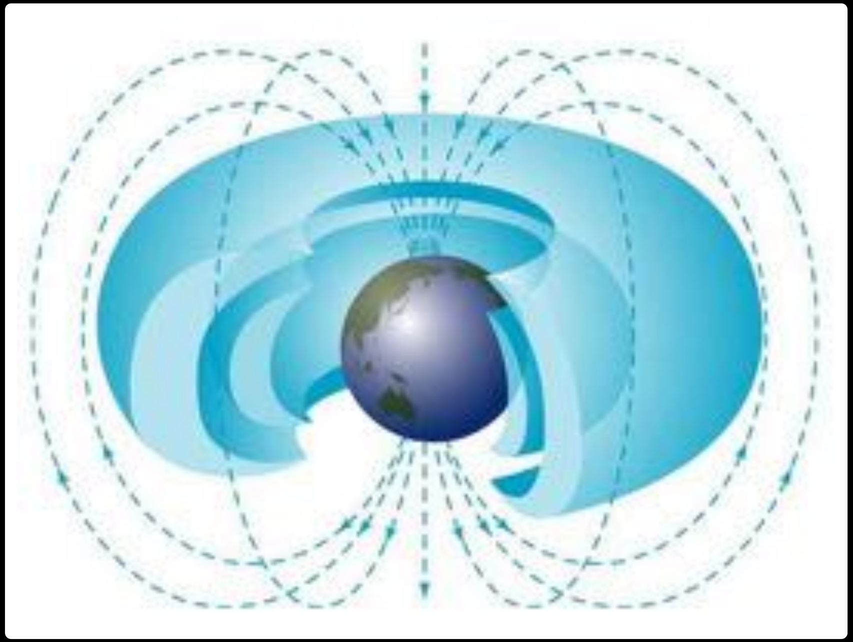

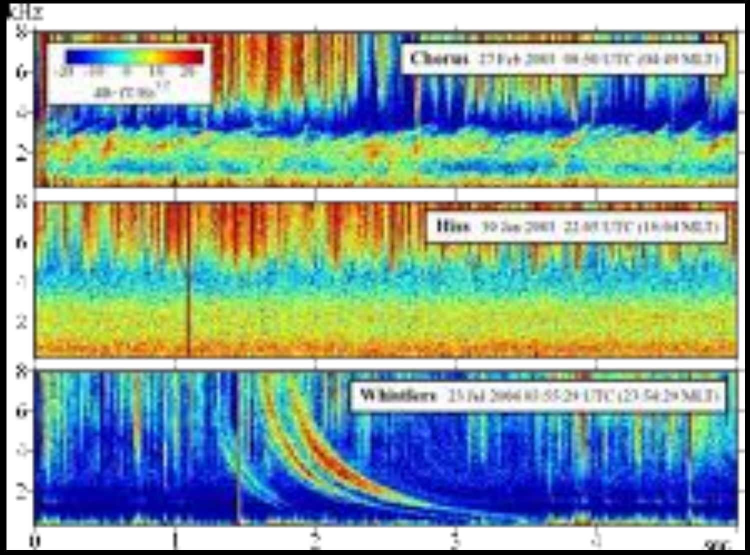

$$PE = 1 - \frac{\sum_{i=1}^{N}(m_i - p_i)^2}{\sum_{i=1}^{N}(m_i - \langle m_i \rangle)^2}.$$

$$\begin{aligned} FS &= \frac{PE_{Model}}{PE_{Persist}} \\ &= \frac{\sum_{i=1}^{N}(m_i - \langle m_i \rangle)^2 - \sum_{i=1}^{N}(m_i - p_i)^2}{\sum_{i=1}^{N}(m_i - \langle m_i \rangle)^2 - \sum_{i=1}^{N}(m_i - m_{i-1})^2}. \end{aligned}$$

$$\begin{aligned} SS &= \frac{PE_{Model} - PE_{Persist}}{1 - PE_{Persist}} \\ &= \frac{\sum_{i=1}^{N}(m_i - m_{i-1})^2 - \sum_{i=1}^{N}(m_i - p_i)^2}{\sum_{i=1}^{N}(m_i - m_{i-1})^2}. \end{aligned}$$

$$SS = \frac{PE_{Persist}(FS - 1)}{1 - PE_{Persist}}.$$

CASE STUDIES

CRRES

Reanalysis from CRRES era

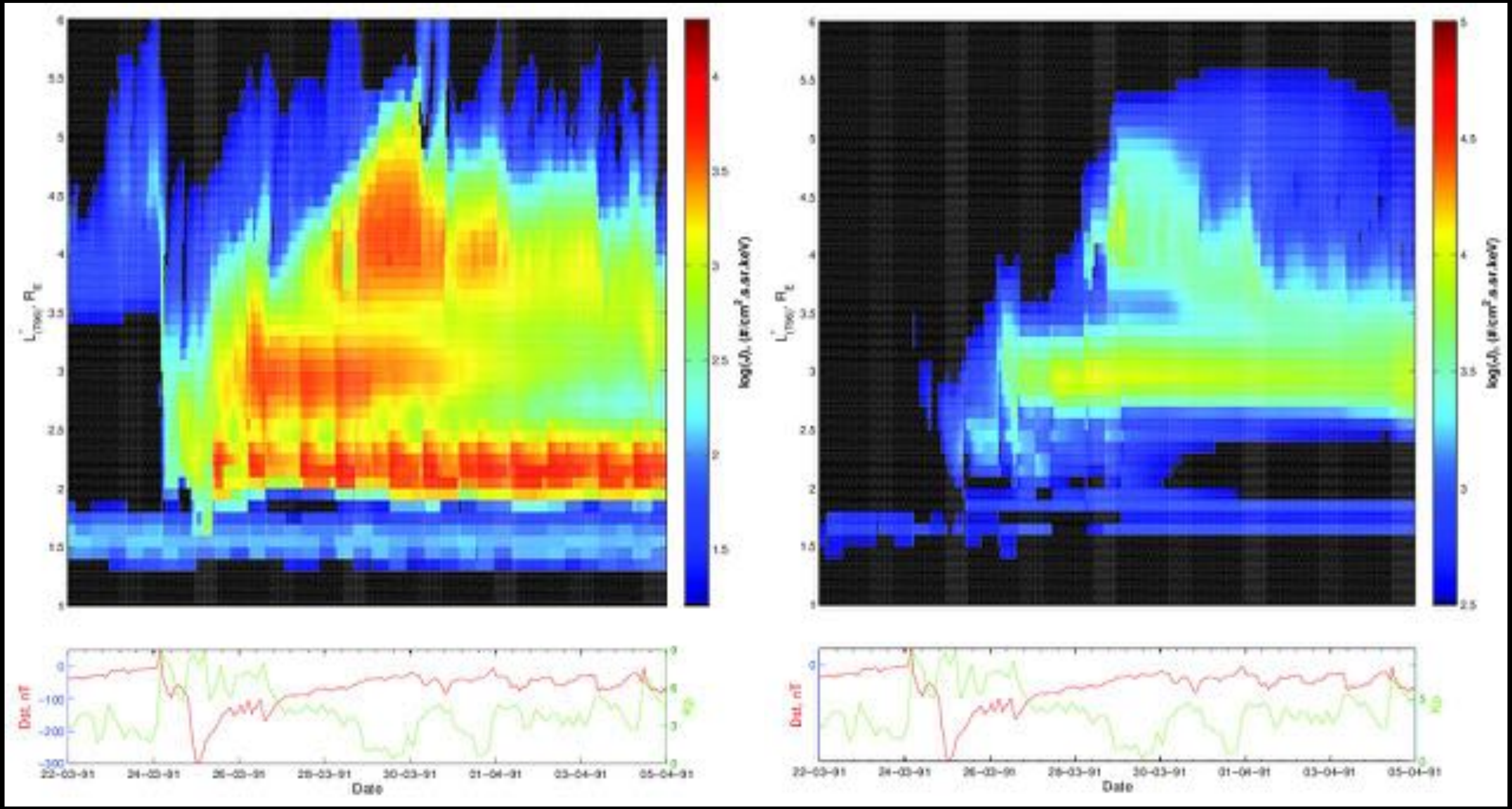

VERB Model

In this study, we use the VERB code 2.0 with the following settings, to simulate radiation belt dynamics.

$$\frac{\partial f}{\partial t} = L^2 \frac{\partial}{\partial L}\Big|_{\mu,J} \frac{1}{L^2} D_{LL} \frac{\partial f}{\partial L}\Big|_{\mu,J} + \frac{1}{p^2}\frac{\partial}{\partial p}\Big|_{\alpha_0,L} p^2 D_{pp} \frac{\partial f}{\partial p}\Big|_{\alpha_0,L} + \frac{1}{T(\alpha_0)\sin(2\alpha_0)}\frac{\partial}{\partial \alpha_0}\Big|_{p,L} T(\alpha_0)$$

Simplified Fokker-Planck

Diffusion coefficients: D_{pp} a

(field-aligned, Gaussian wa

plasmaspheric hiss)

$$D_{LL} = 10^{0.056Kp - 9.325} L^{10}.$$

[Brautigam and Albert, 200

Wave Parameters:

Wave type	$B_w (pT)$	λ_{max}, °	Ratio of plasma to gyrofrequency	MLT (%)	Wave spectral properties
Chorus day	$10^{0.75+0.04\lambda}$	35	$N_0 = 124 \cdot (3/L)^4$, [a] $\omega_p = \sqrt{4\pi N_0 q_e^2/m}$ $f = \frac{\omega_p}{\Omega_e}$	25	$\omega_m/\Omega_e = 0.2$, $\delta\omega/\Omega_e = 0.1$, $\omega_{uc}/\Omega_e = 0.3$, $\omega_{lc}/\Omega_e = 0.1$
Chorus night	50	15	$N_0 = 124 \cdot (3/L)^4$, [a] $\omega_p = \sqrt{4\pi N_0 q_e^2/m}$ $f = \frac{\omega_p}{\Omega_e}$	25	$\omega_m/\Omega_e = 0.35$, $\delta\omega/\Omega_e = 0.15$, $\omega_{uc}/\Omega_e = 0.65$, $\omega_{lc}/\Omega_e = 0.05$
Hiss inside plasmasphere	30	40	$N_0 = 10^{-0.3145L+3.9043}$, [b] $\omega_p = \sqrt{4\pi N_0 q_e^2/m}$ $f = \frac{\omega_p}{\Omega_e}$	60 [c]	$\omega_m = 3587 rad/sec$, $\delta\omega = 1797 rad/sec$, $\omega_{uc} = 12566 rad/sec$, $\omega_{lc} = 628, rad/sec$

Table 2.1: Wave parameters used for computing pitch angle and energy diffusion coefficients

(a)[*Sheeley et al.*, 2001] (b)[*Carpenter and Anderson*, 1992] (c)[*Meredith et al.*, 2006]

VERB Model

Boundary conditions are as indicated to right, except for outer boundary. We use L = 6 and update outer boundary PSD from reanalysis from previous time step.

Boundary	Condition	Explanation
$E = E_{min}$	$f = const$	Balance of convective source and losses
$E = E_{max}$	$f = 0$	Absence of high energy electrons at multi-MeV energies
$\alpha_0 = 0°$	$f = 0$	Empty loss cone in the week diffusion regime
$\alpha_0 = 90°$	$\partial f / \partial \alpha_0 = 0$	Flat pitch angle distribution at 90°
$L = 1$	$f = 0$	Losses to atmosphere
~~$L = 7$~~	~~$f = f(time)$~~	~~Measurements~~

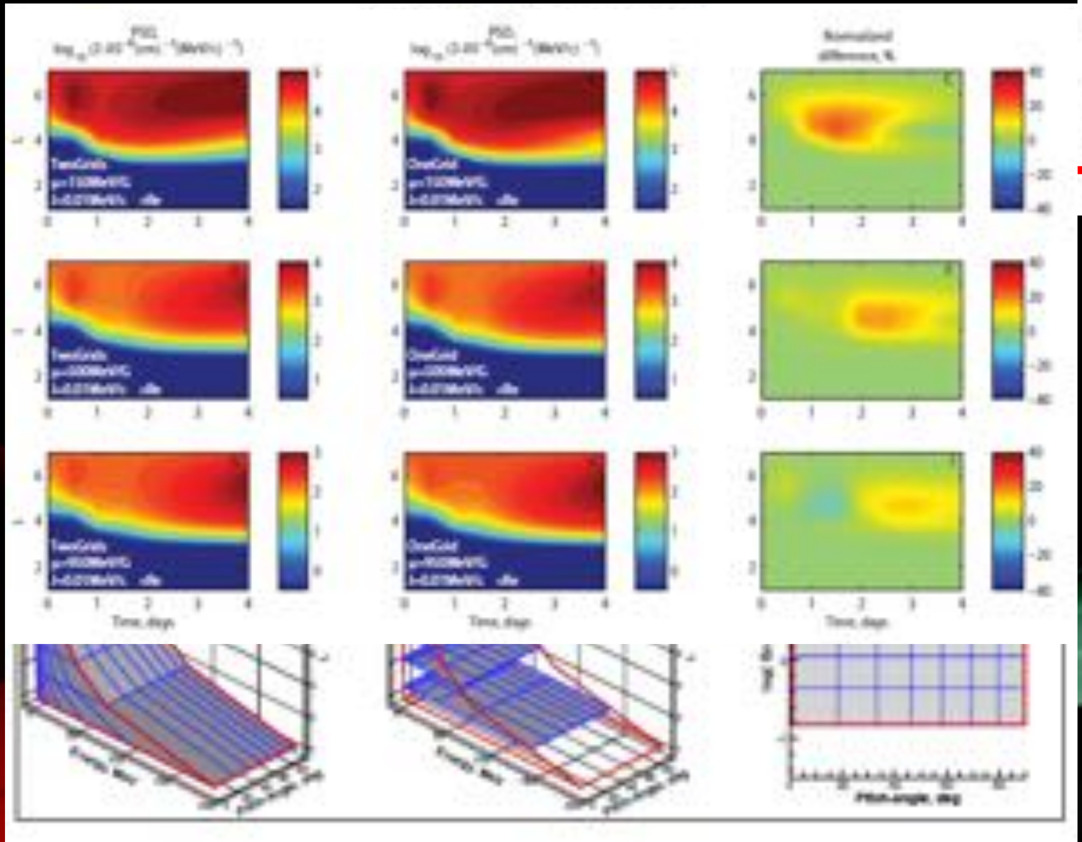

We use a simplified single grid. (L, μ, α), which is correct within wave parameterization error ~30%, provided the grid is large enough, time step is small enough, and we use a logarithmic energy grid.

[Subbotin and Shprits, 2009]

Radiation Belt Forecast Framework

http://rbm.epss.ucla.edu/realtime-forecast/

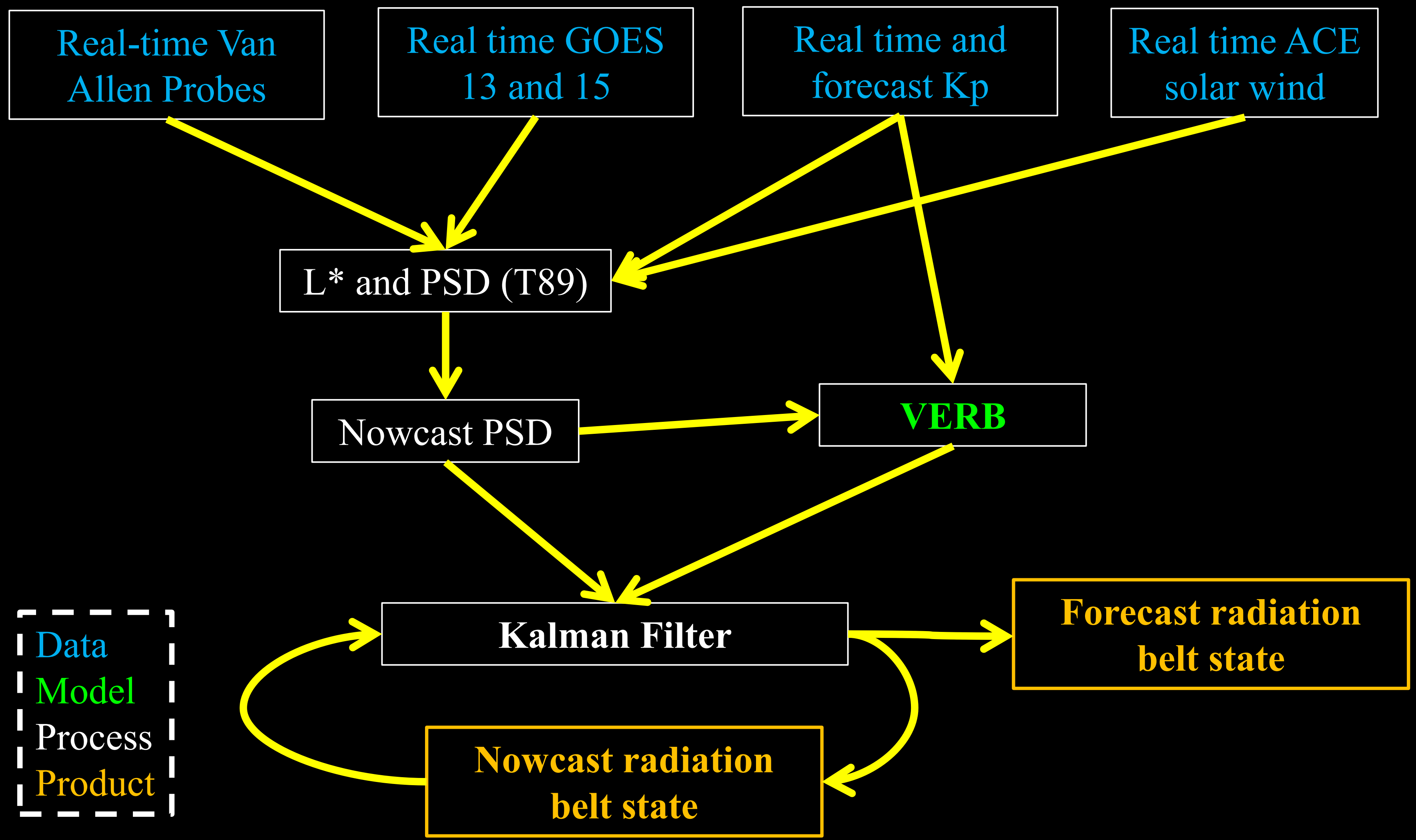

Reanalysis and Forecasting

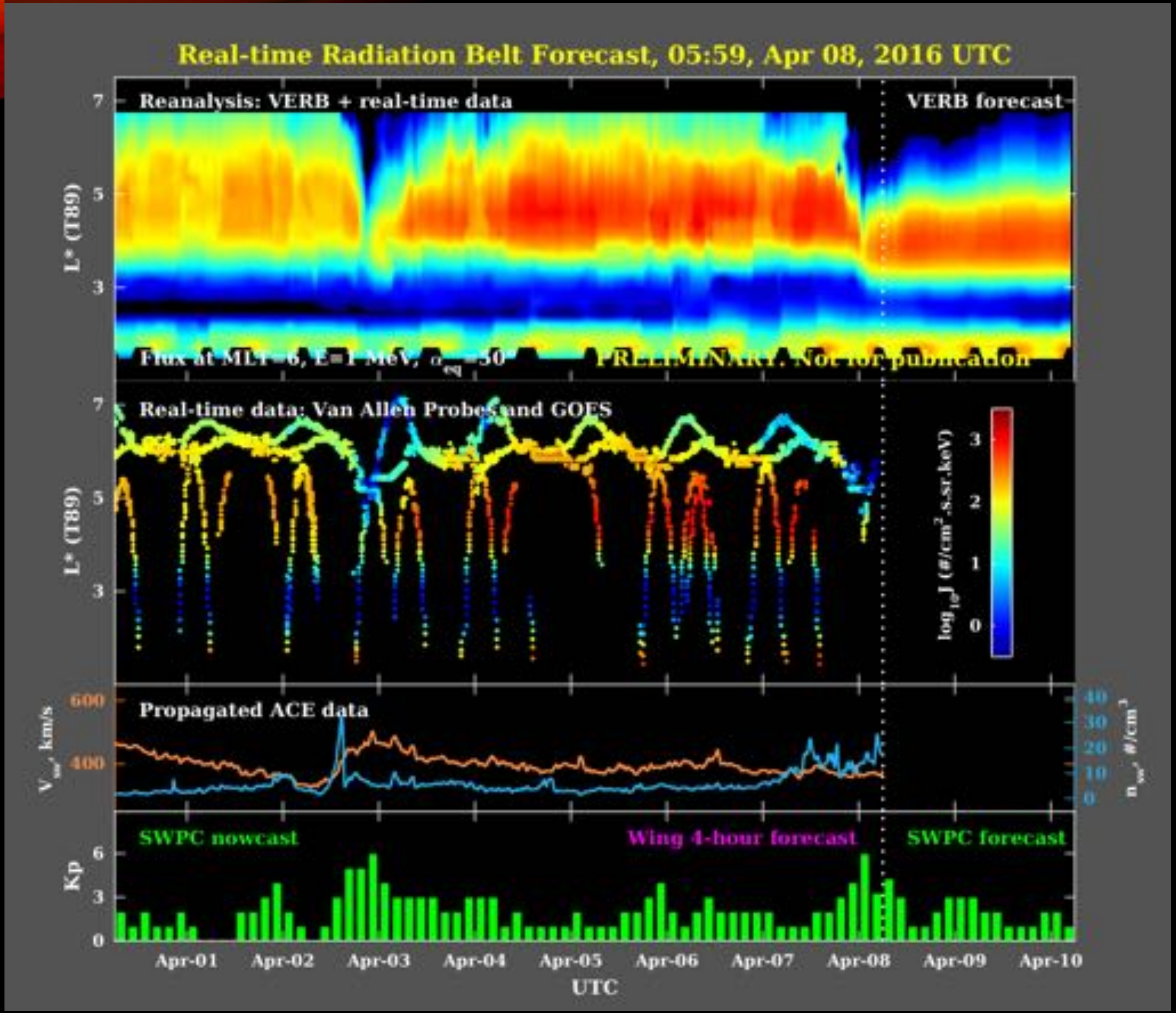

Recent example of radiation belt forecast fluxes at 1 MeV

The forecast runs every 2 hours automatically, and the most recent forecast figure is shown at the following web address

http://rbm.epss.ucla.edu/realtime-forecast/

Forecast Performance

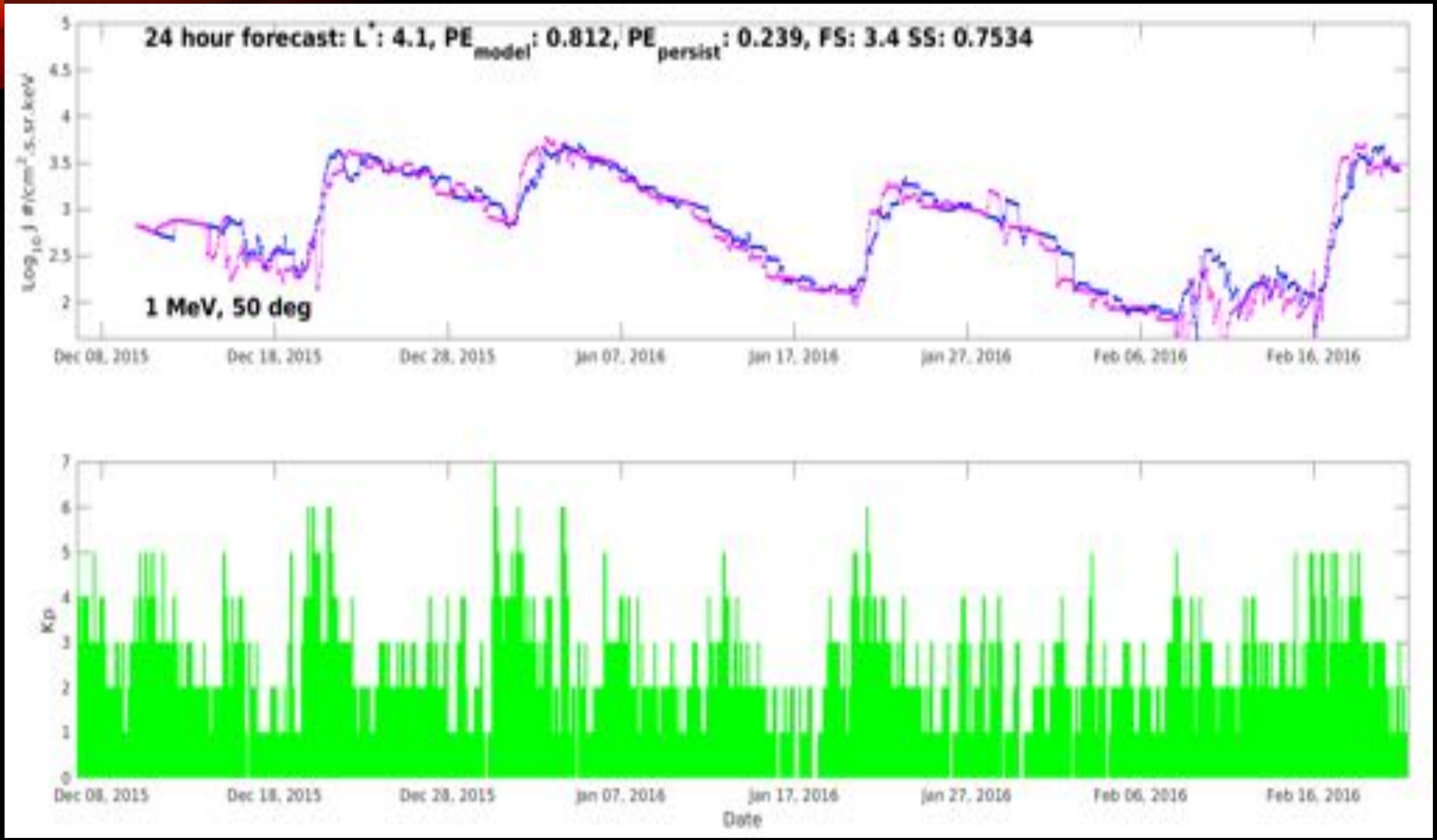

Kellerman et al., [2016], Space Weather – in preparation

$$SS = \frac{PE_{Model} - PE_{Persist}}{1 - PE_{Persist}} = \frac{\sum_{i=1}^{N}(m_i - m_{i-1})^2 - \sum_{i=1}^{N}(m_i - p_i)^2}{\sum_{i=1}^{N}(m_i - m_{i-1})^2}.$$

Forecast Performance

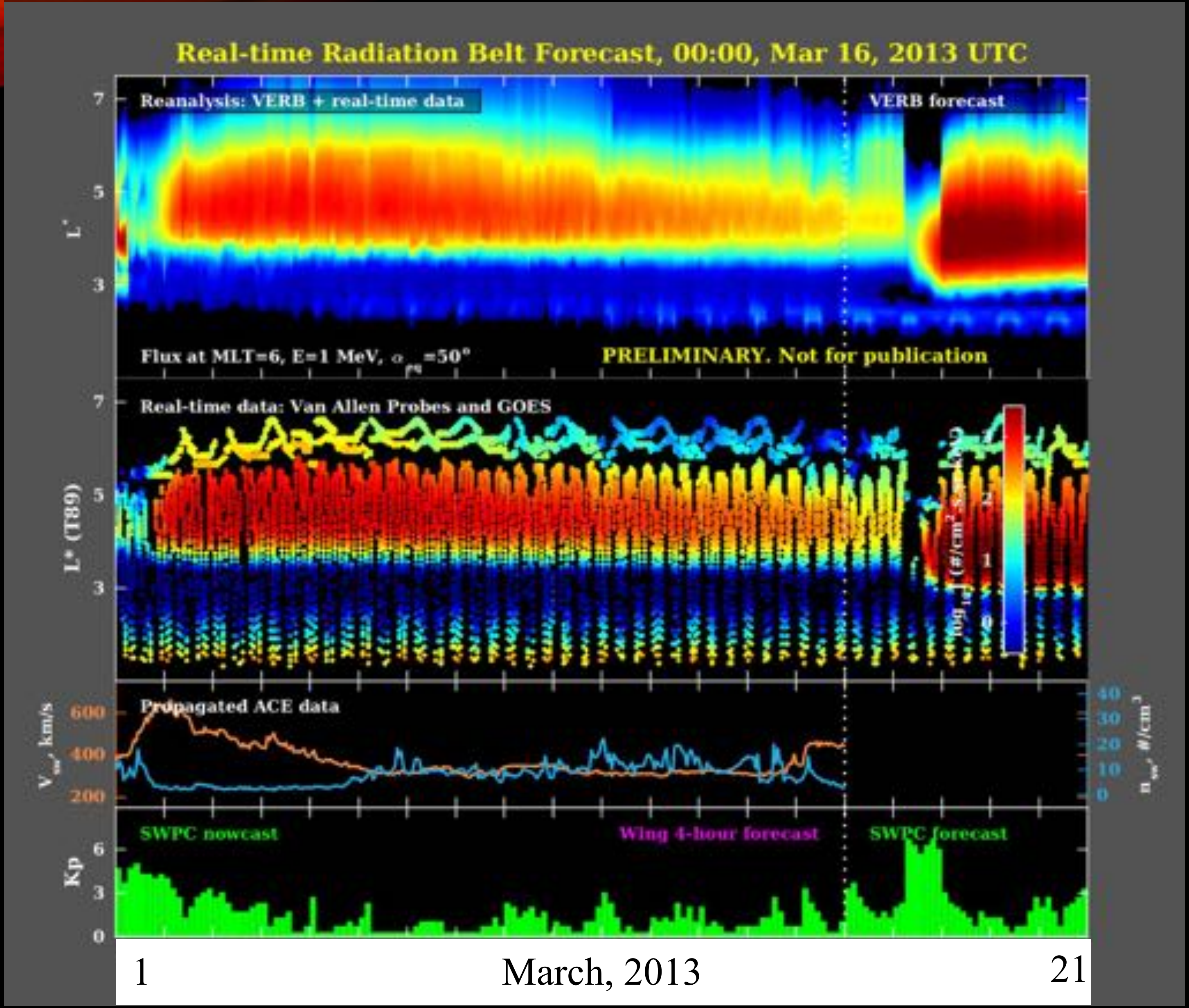

The B-field model is important!

Diffusion Coefficients

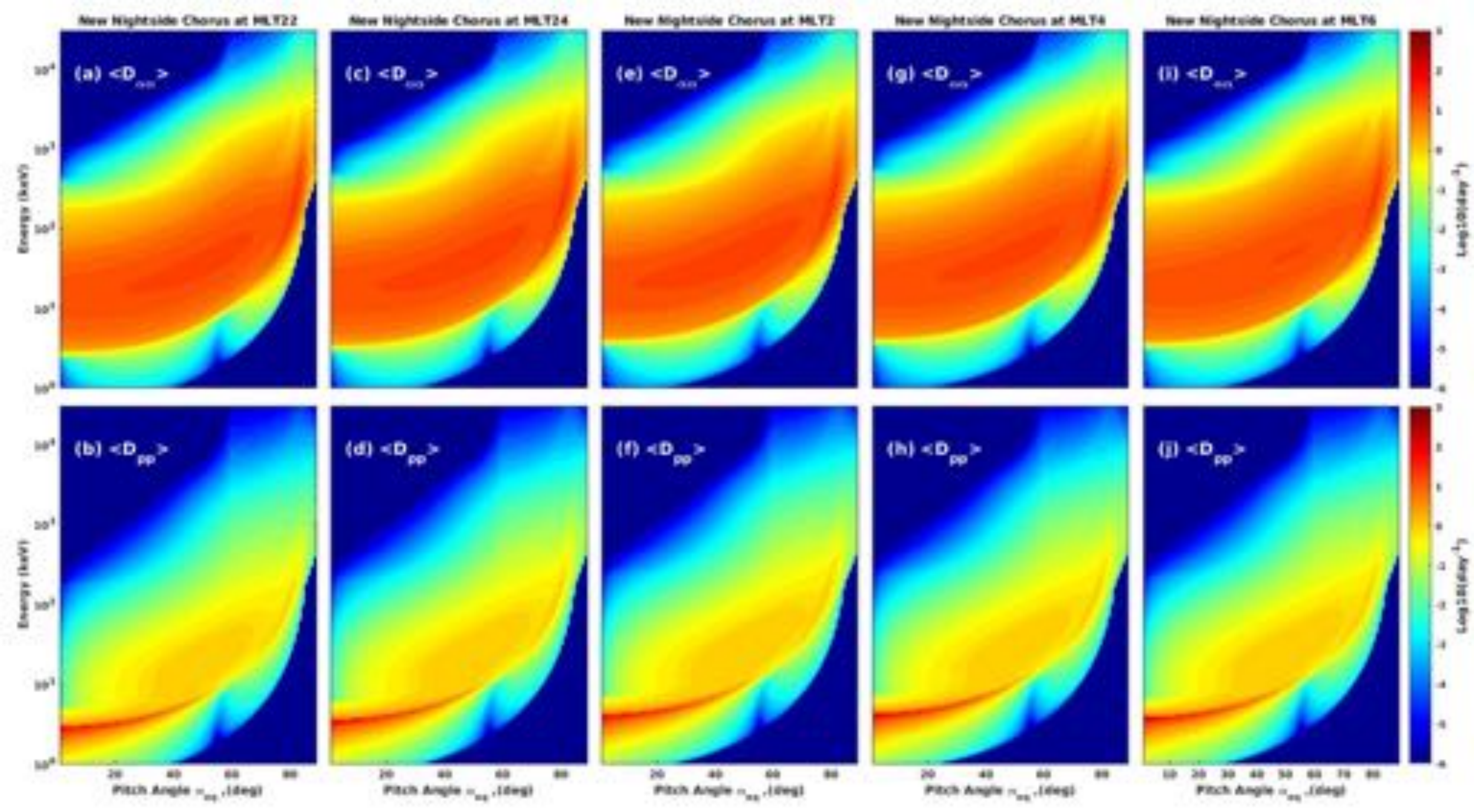

Hui Zhu - Friday 4pm – GEM, QARBM

Diffusion Coefficients

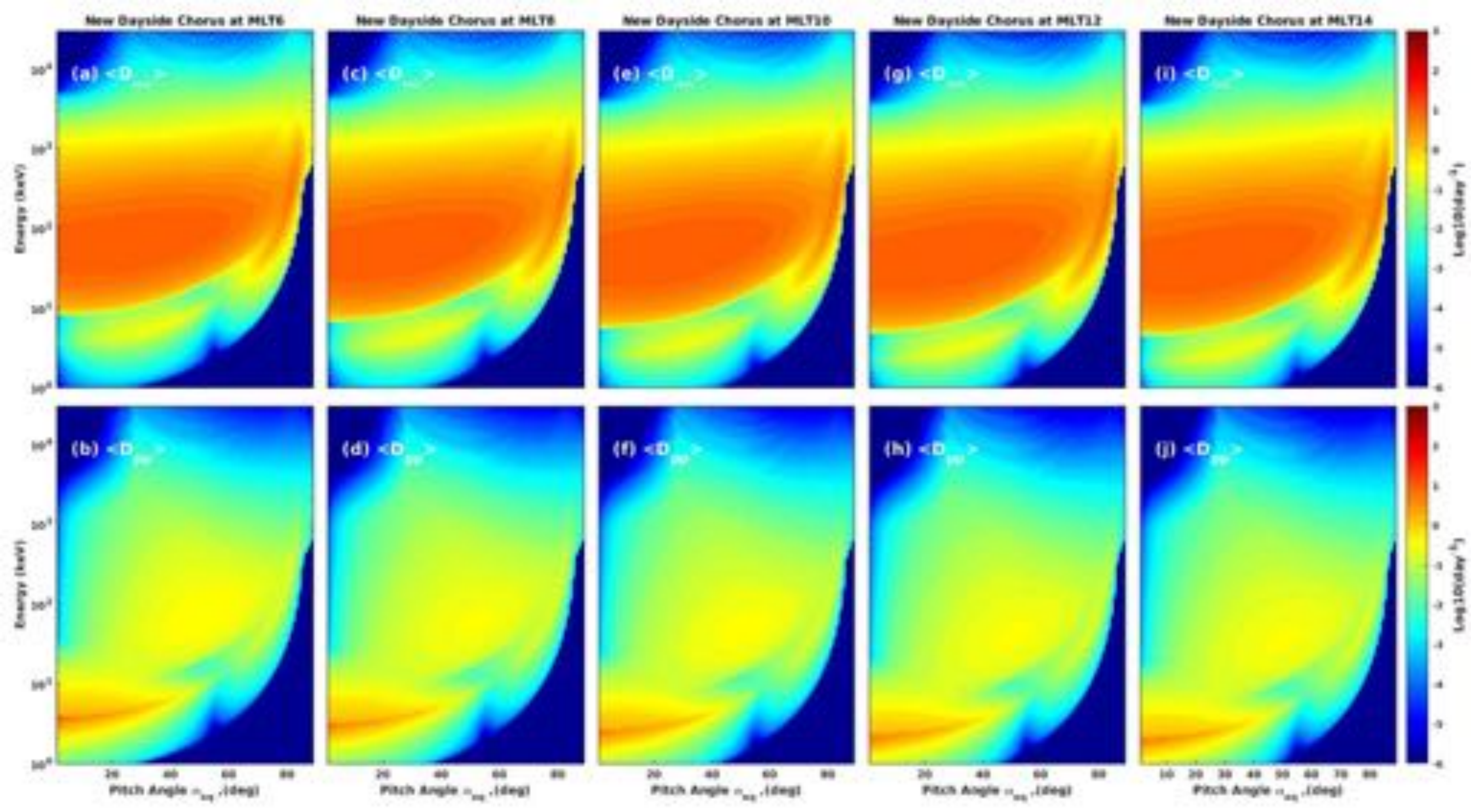

DA BACKUP

Kalman Filter

X: State vector, PSD $(c/(cm.MeV))^3$
M: Model matrix (VERB code)
P: State error covariance matrix
Q: Model covariance matrix.
y: PSD measurements
K: Kalman Gain
R: Measurement error

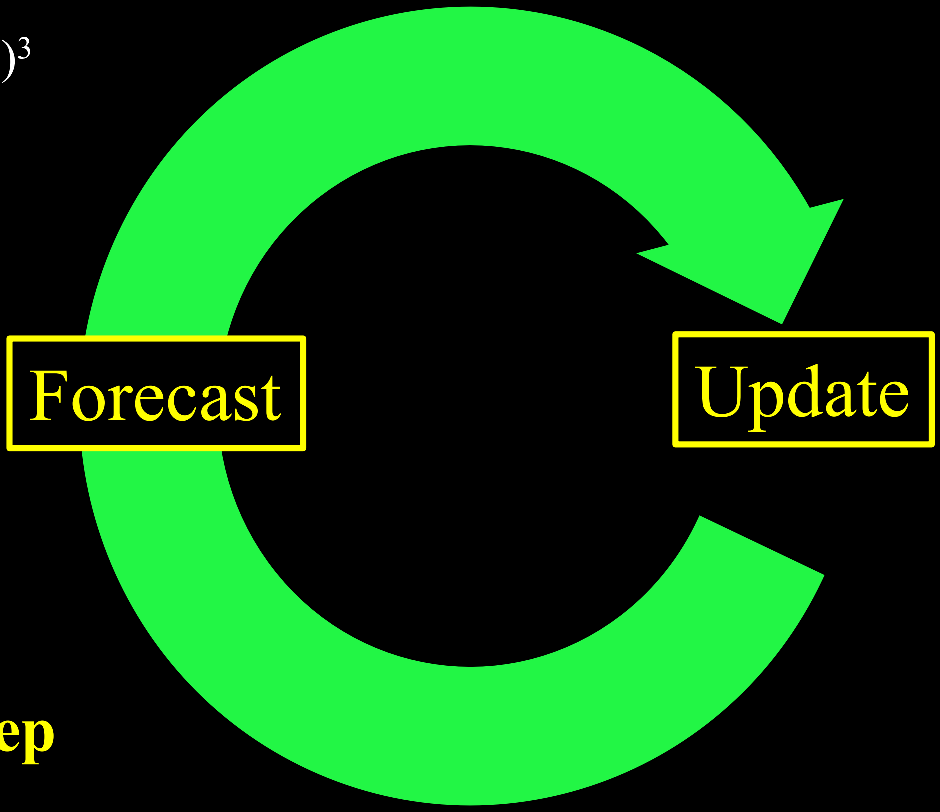

Forecast Step:

$$X_f = M_t X_{t-1|}$$

$$P_f = M_t P_{t-1} M_t^T + Q_t$$

Update Step

$$X_a = X_f + K_t (y_t - X_f)$$

$$K_t = P_f (P_f + R_t)^{-1}$$

$$P_a = (I - K_t) P_f$$

Observational error and bias

We set out to minimize:

$$\Delta PSD_{21} = 2(c_f \times PSD_2 - PSD_1)/(c_f \times PSD_2 + PSD_1)$$

PSD at fixed L*, μ, and K.

PSD_1 is the reference or gold standard
c_f is a calibration coefficient

$\Delta L^* \leq 0.1 R_E$ $\Delta t \leq 5\,\text{min}$

Find c_f that minimizes the mean ΔPSD for each fixed invariant pair

Use the weighted mean of c_f for all L* and K conjunctions to correct each energy channel, and estimate the bias. The width of the distribution gives an estimate of the error between the two spacecraft.

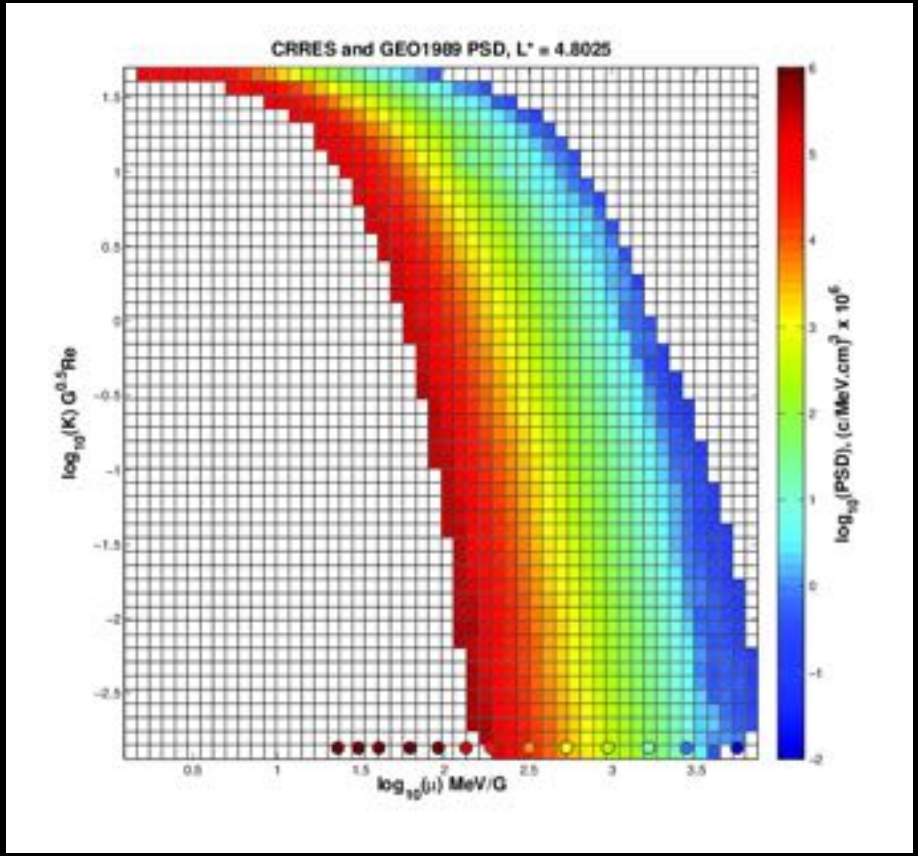

Observational error and bias

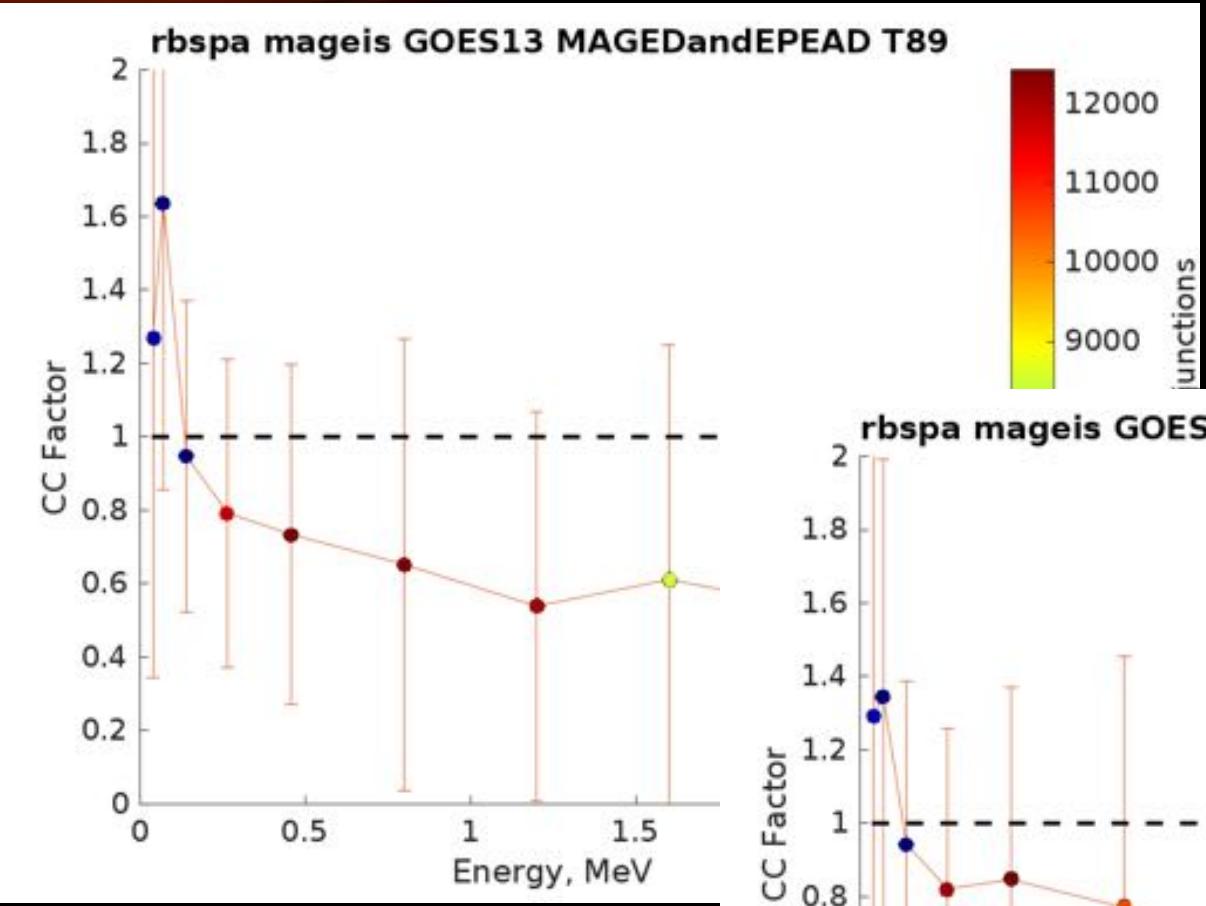

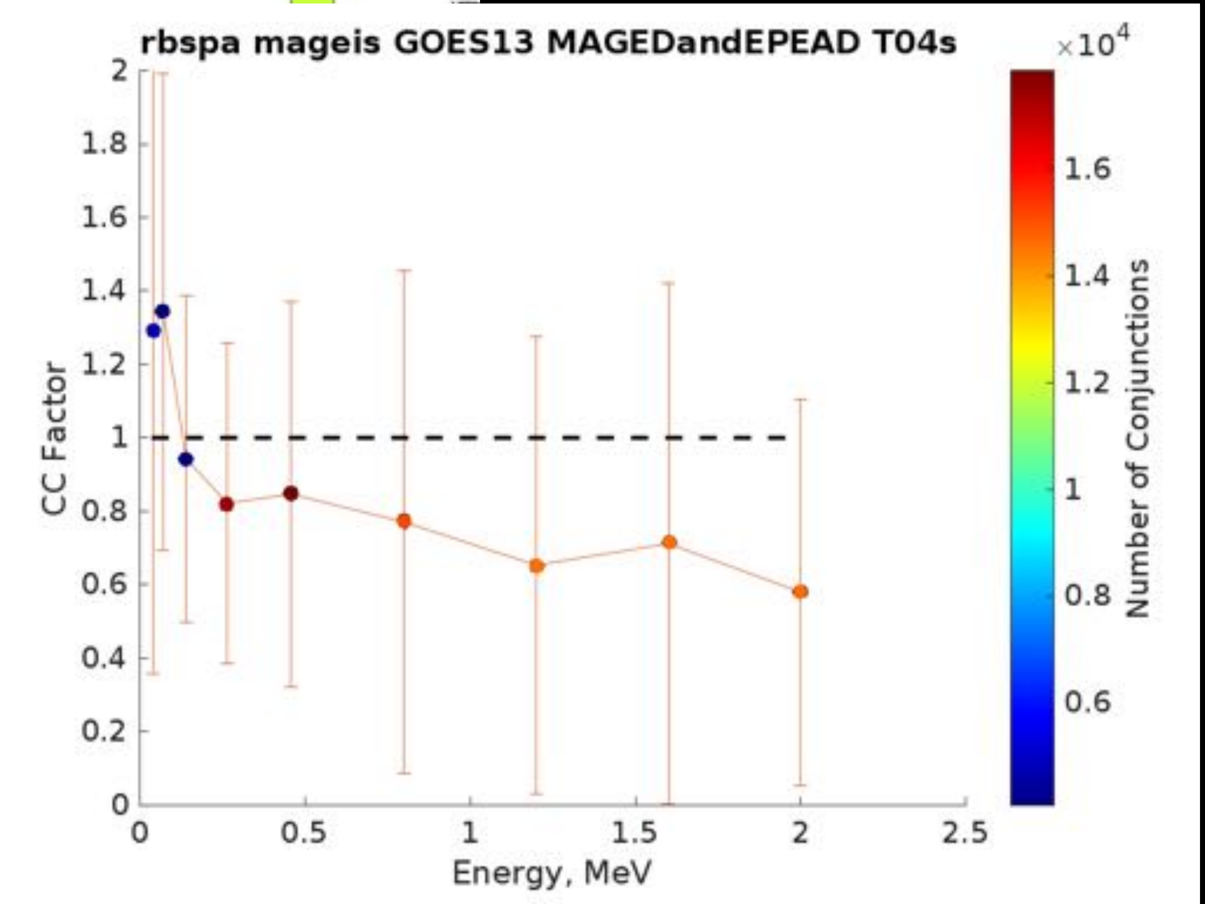

Background March 1991

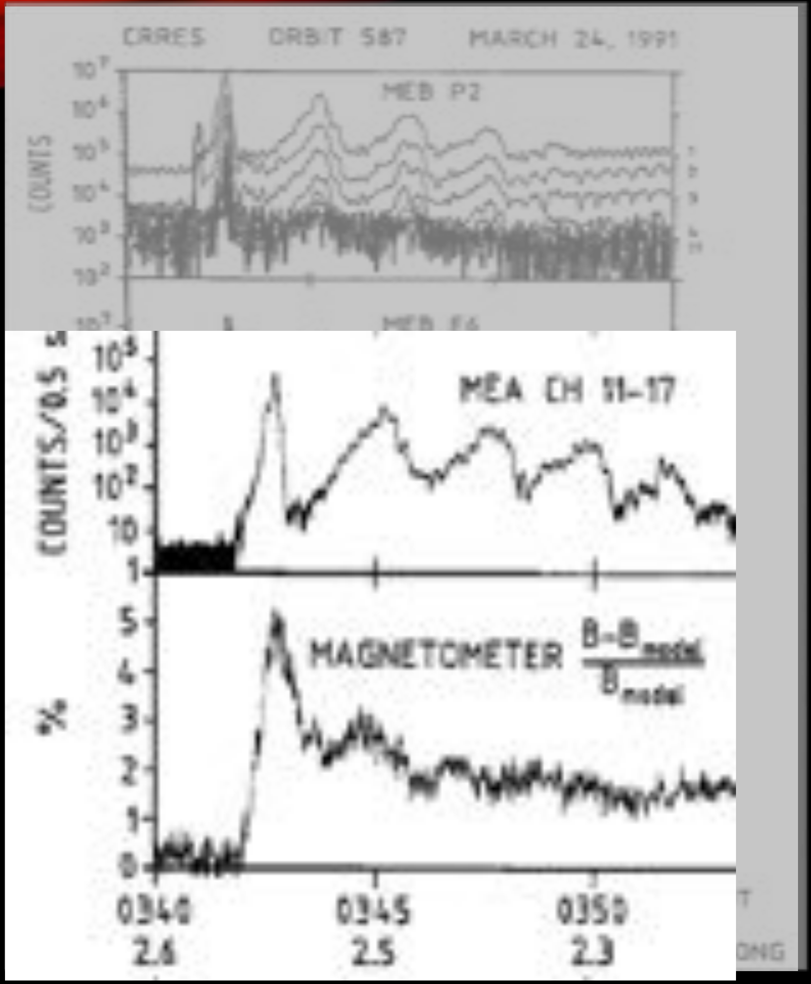

Vampola,and Korth [1992]

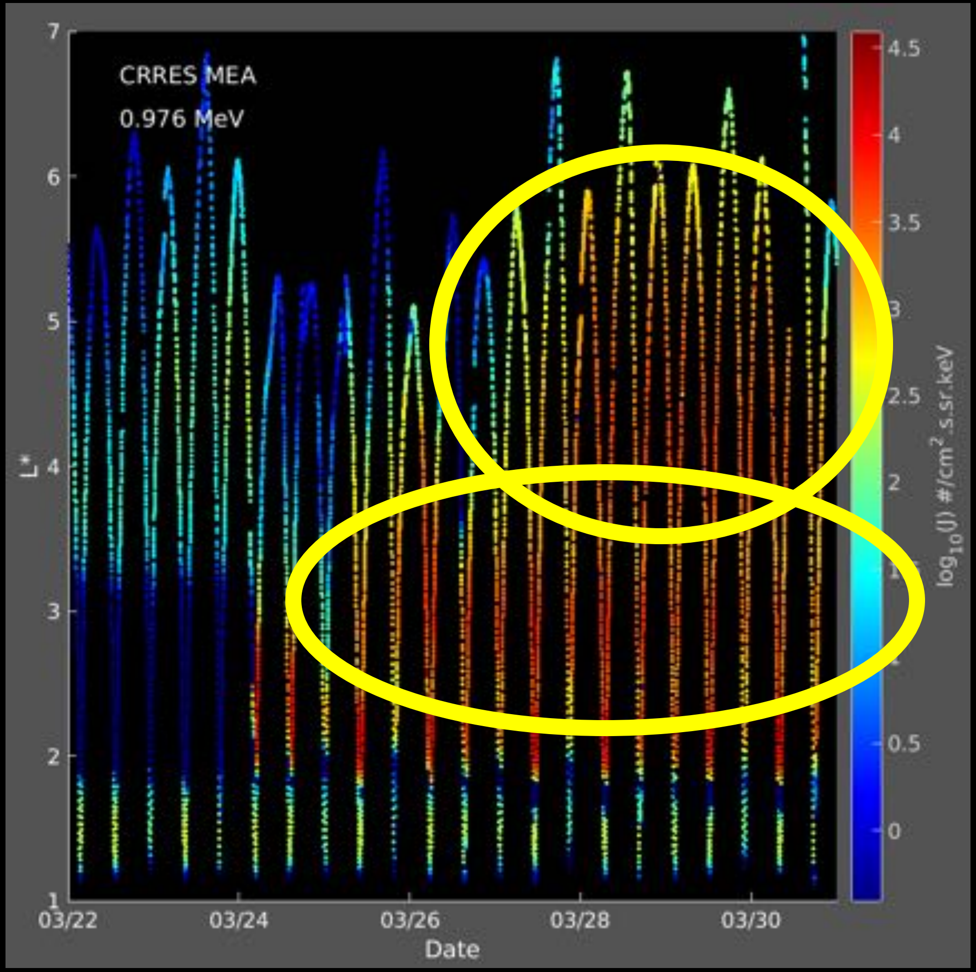

In this study, we focus on two enhancements in electron flux observed during the same storm

Observations

We include 5 Spacecraft:

CRRES - HAEO

Akebono - LEO

GPSns18 - MEO

GEO1989 - GEO

GEO1990 - GEO

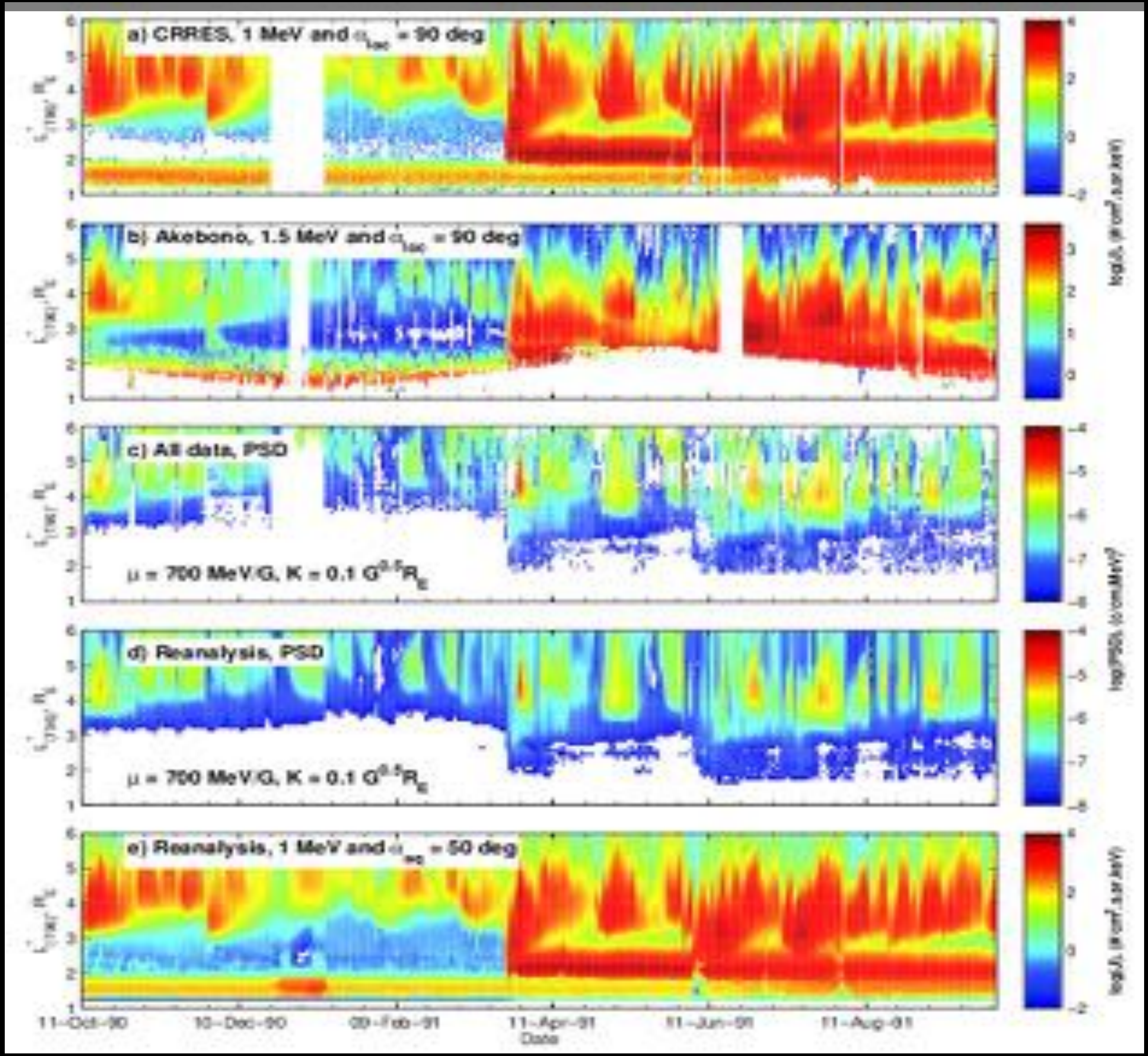

The Third Radiation Belt

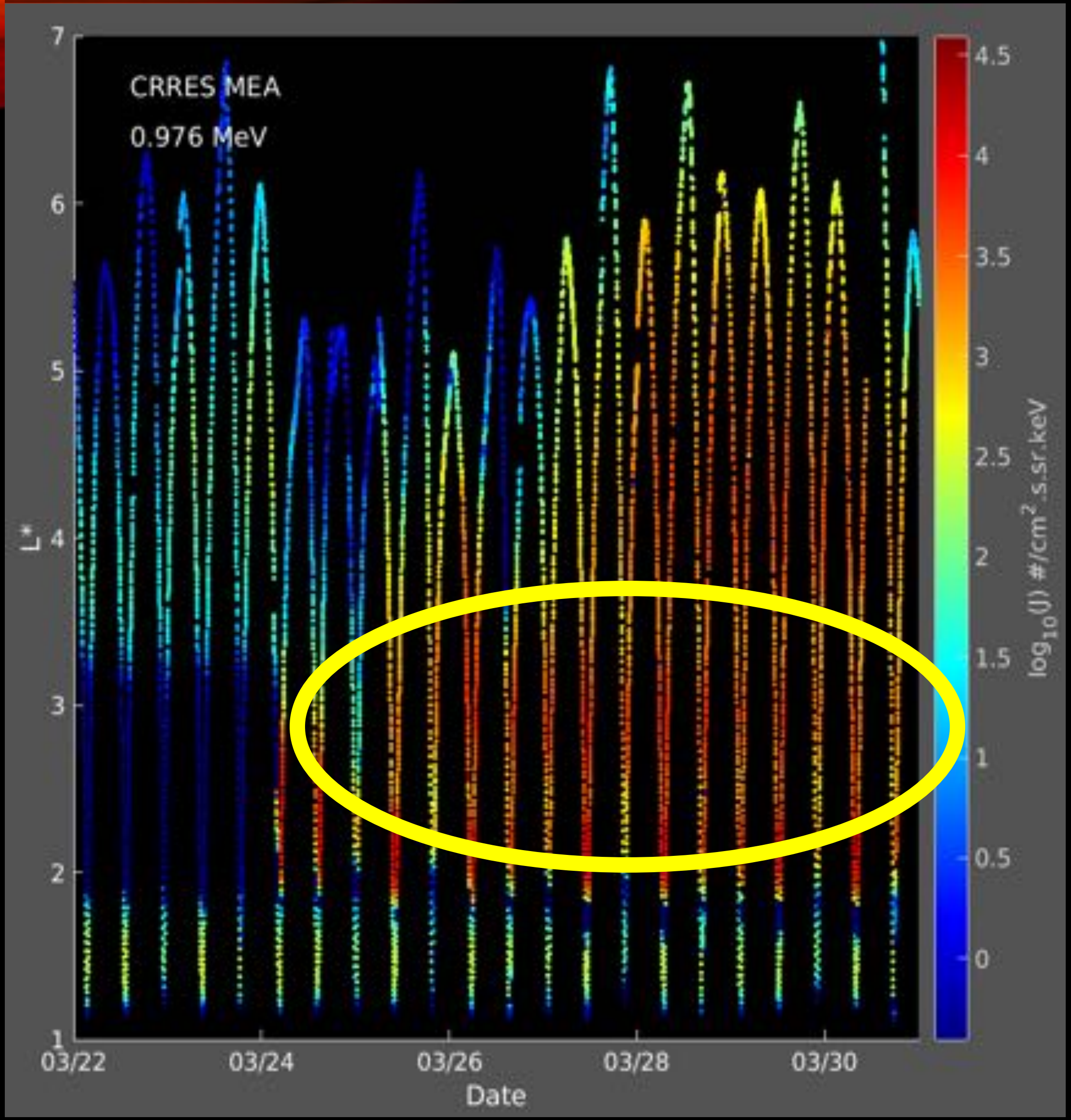

CRRES was located pre-midnight at 23.5 MLT and near L* = 4 during this period

a) Flux increases across all energies early on March 26

b) Adiabatic above ~0.4 MeV, and non-adiabatic below.

c) Evidence of dipolarization in Bz

Evidence of a particle injection.

The Fourth Radiation Belt

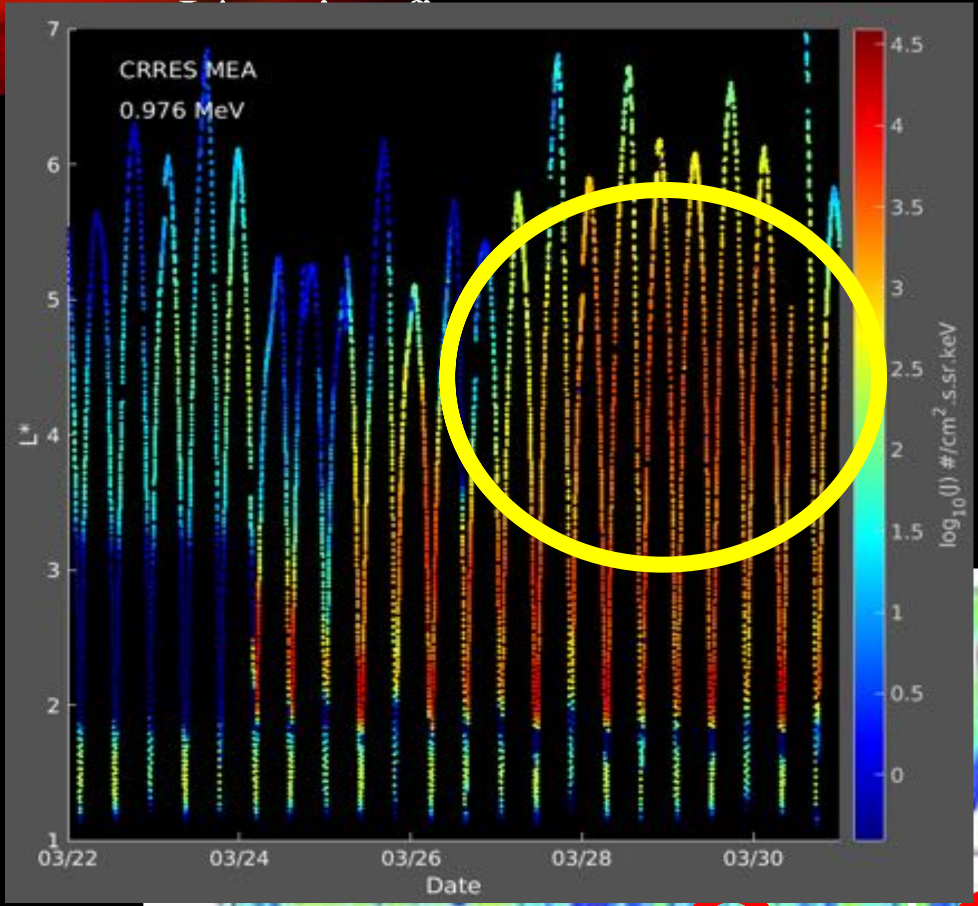

We usually consider L* vs time figures of PSD at fixed μ and K

Peaks in PSD at a particular L* represent either local acceleration or variable boundary effects. [*Selesnick and Blake*, 2000]

In 3D reanalysis we reconstruct the PSD globally, over a complete grid of, L*, μ, and K

In order to inve tig SD evolution over various μ in L* on plot a set of snapshot figures, each fo a fi K and time

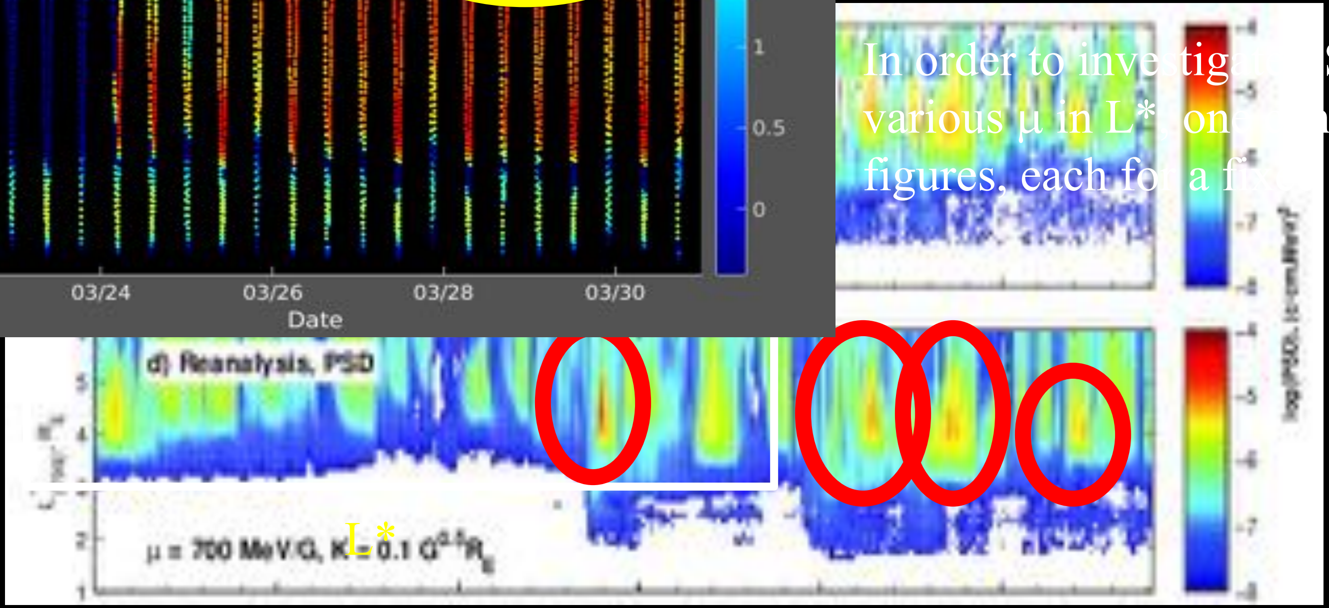

μ,

L*

PSD Analysis

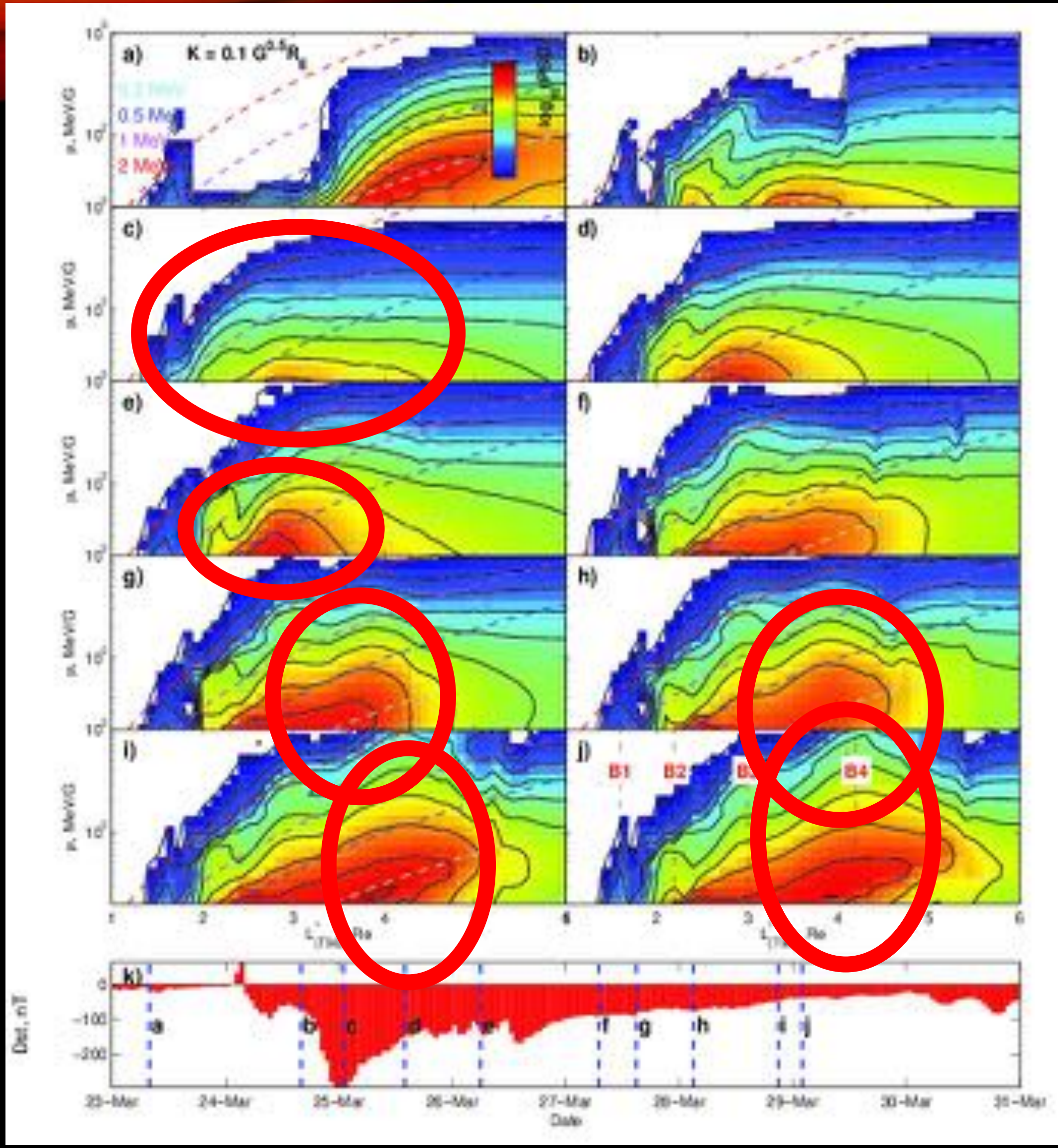

Each panel represents a snapshot, indicated by the blue dashed lines in panel (k)

1) Rapid loss during the main phase

2) The appearance of a third radiation belt

3) Growing peaks in PSD to form a fourth belt

The growing peaks in PSD indicate that the fourth belt was created by local acceleration.

Kellerman et al., [2014], JGR

4-Zone Structure

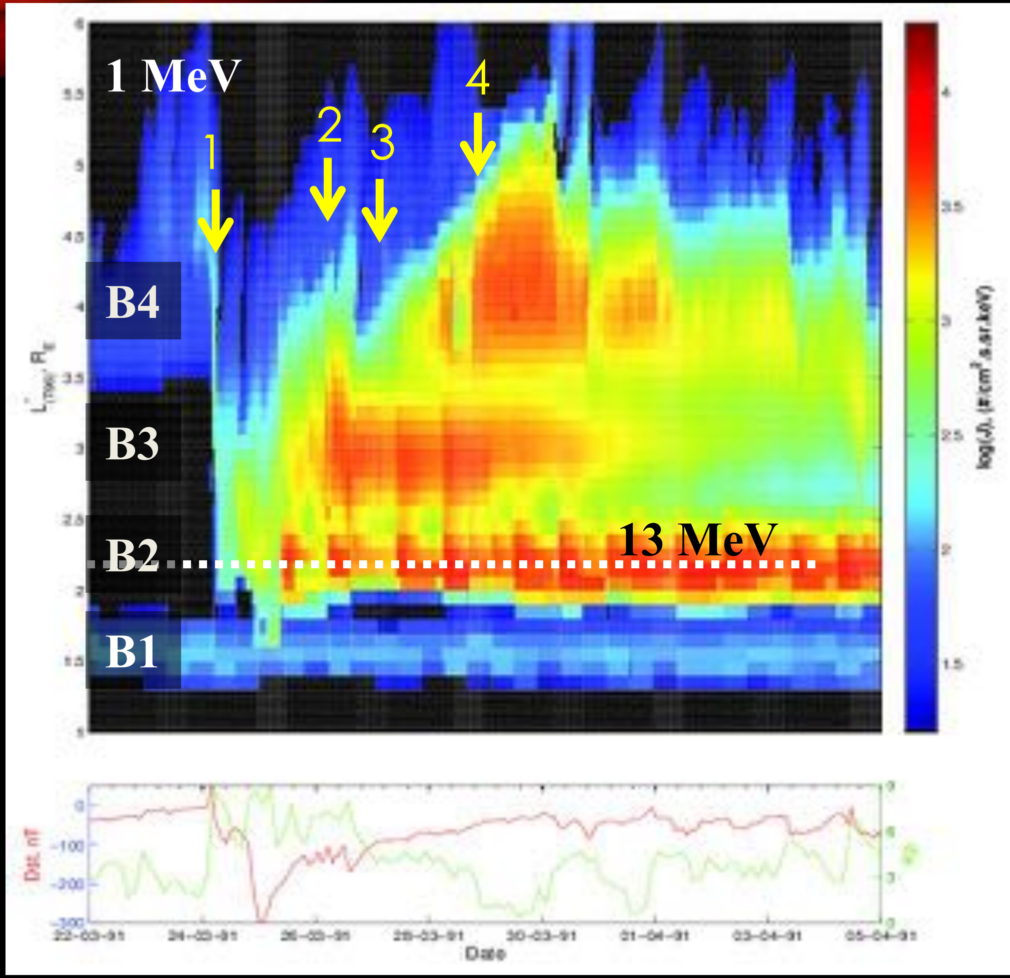

There are 4 mechanisms that resulted in the observed four-zone structure

1. Prompt injection
2. Secondary injection
3. Losses/outward radial diffusion
4. Local acceleration

Reanalysis dataset including LCDS

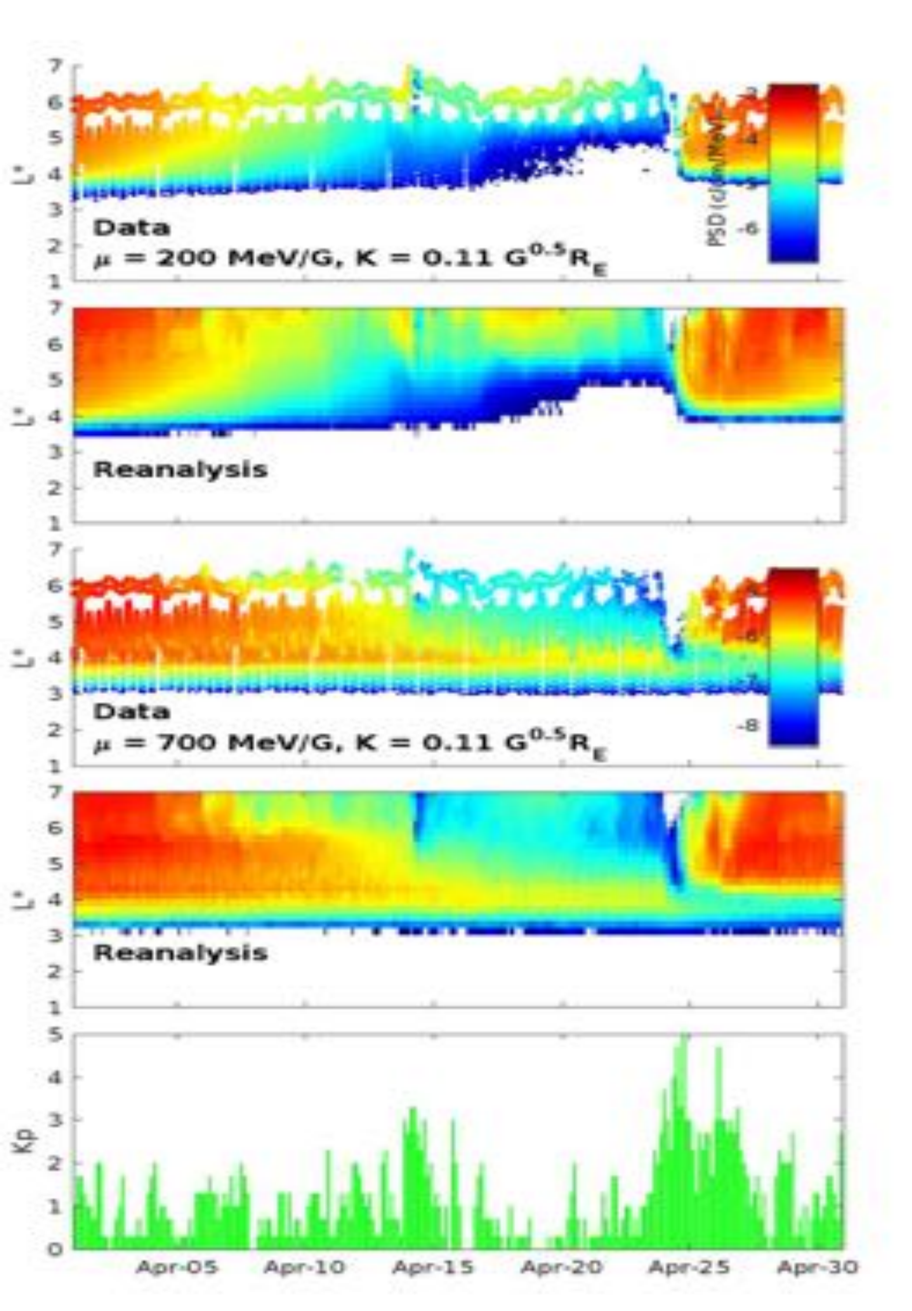

Van Allen Probe and GOES data, now including losses to the magnetopause based on the last-closed-drift shell (LCDS)

Invariant coordinates are based on T89, T04s and TS07D-1A

The LCDS is currently based on T04s

The dataset spans Oct 2012 – Oct 2016

LCDS work with Steve Morley and Jay Albert (LANL/AFRL)

TS07D model work with Grant Stephens and Misha Sitnov (APL)

Integration into IRBEM with Paul O'Brien (Aerospace) and Sebastian Bourdarie (ONERA)

1D Data Assimilation

First application to our 1D-radial diffusion model $\frac{\partial f}{\partial t} = L^2 \frac{\partial}{\partial L}\Big|_{\mu,J} \frac{1}{L^2} D_{LL} \frac{\partial f}{\partial L}\Big|_{\mu,J}$ $-f/\tau$

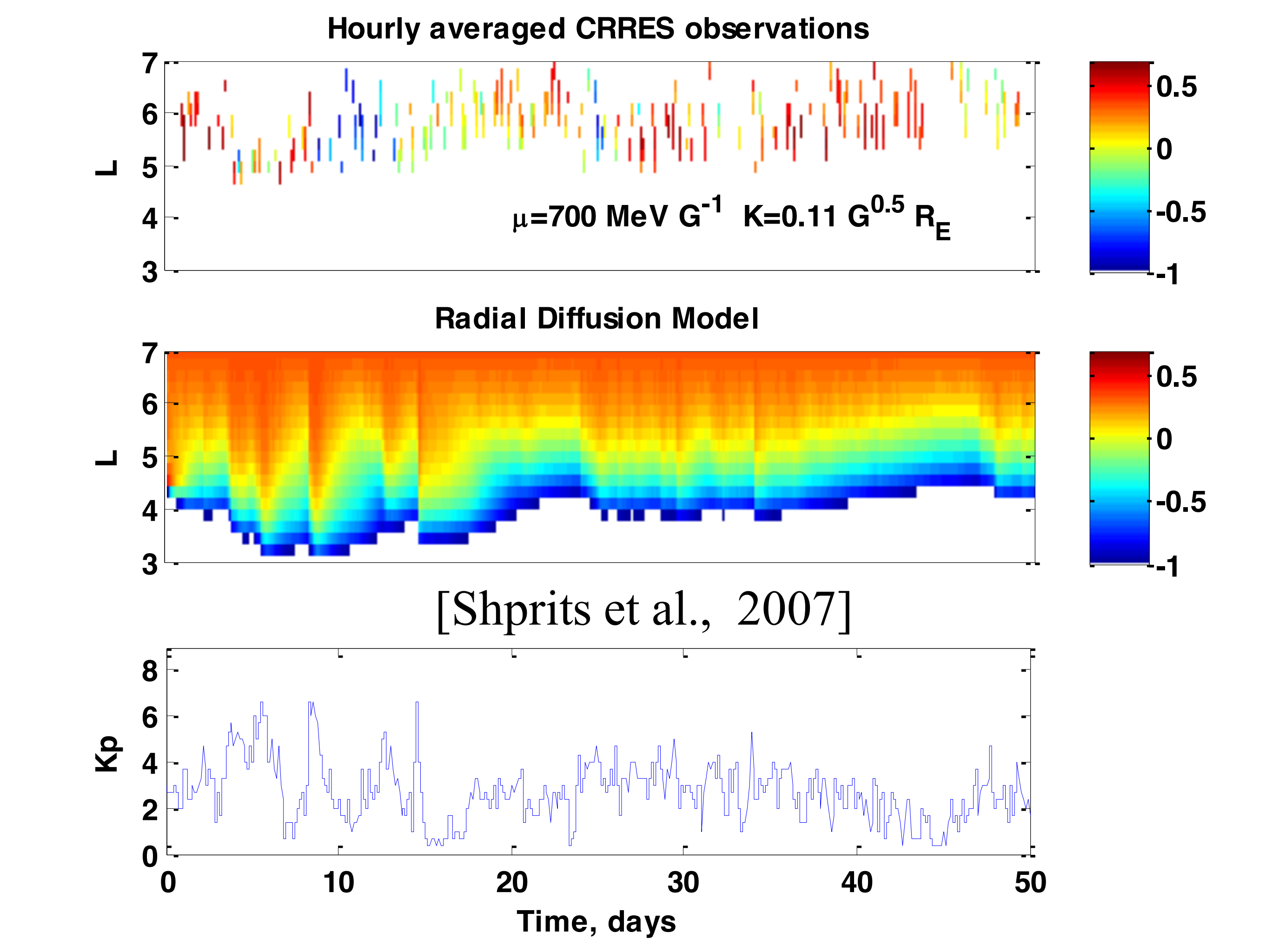

[Shprits et al., 2007]

1D Data Assimilation

First application to our 1D-radial diffusion model $\frac{\partial f}{\partial t} = L^2 \frac{\partial}{\partial L}\Big|_{\mu,J} \frac{1}{L^2} D_{LL} \frac{\partial f}{\partial L}\Big|_{\mu,J}$ $-f/\tau$

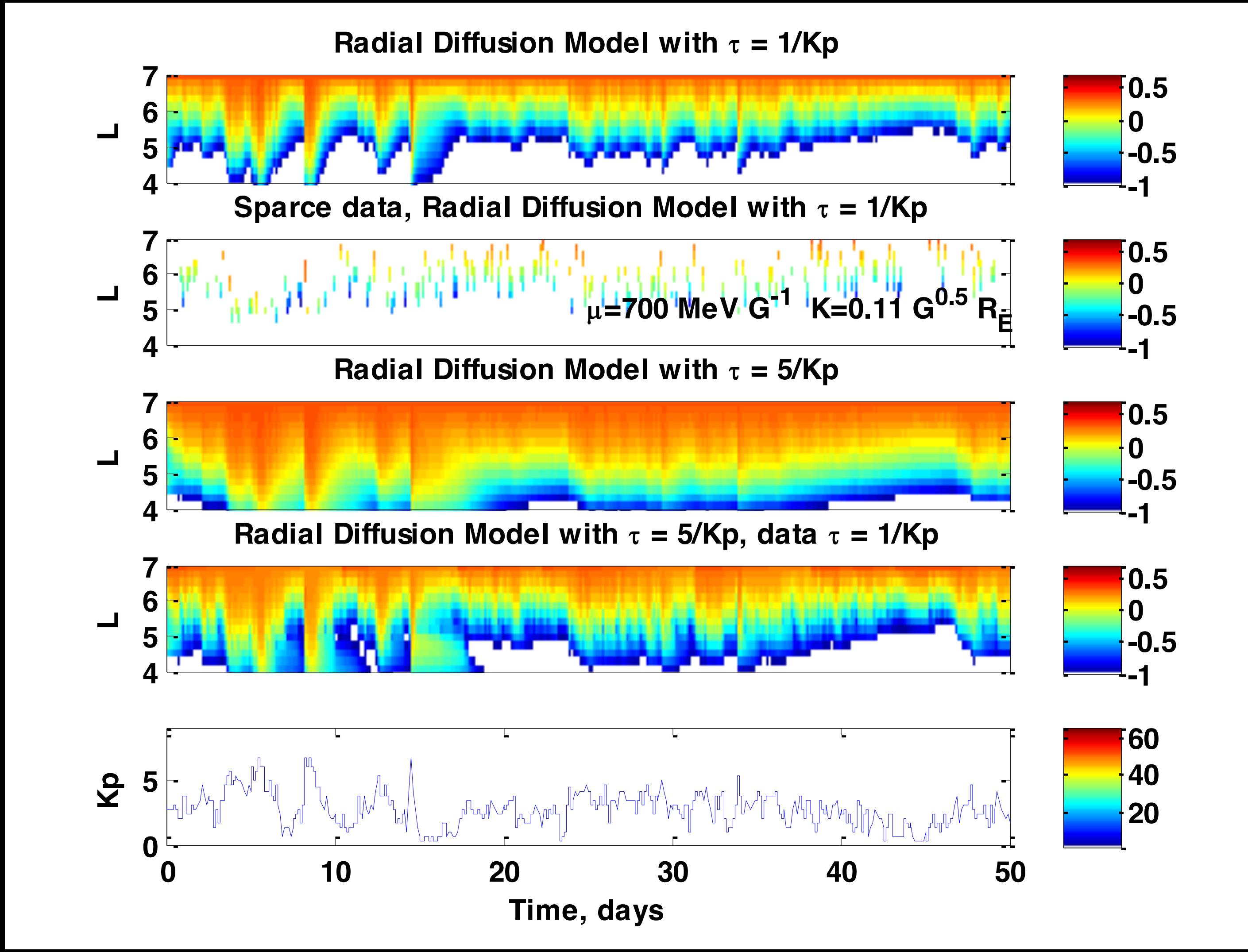

1D Data Assimilation

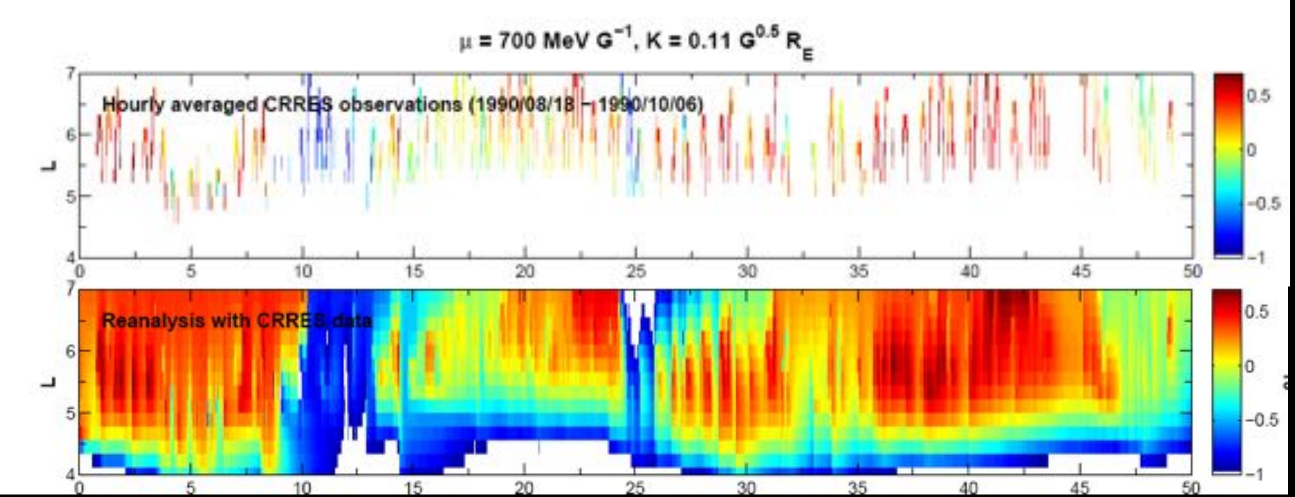

Persistent peaks in PSD and positive innovation indicate that in addition to the radial diffusion there is another acceleration mechanism present in the inner magnetosphere.

Negative innovation at the outer L-shells may indicate an additional loss mechanism.

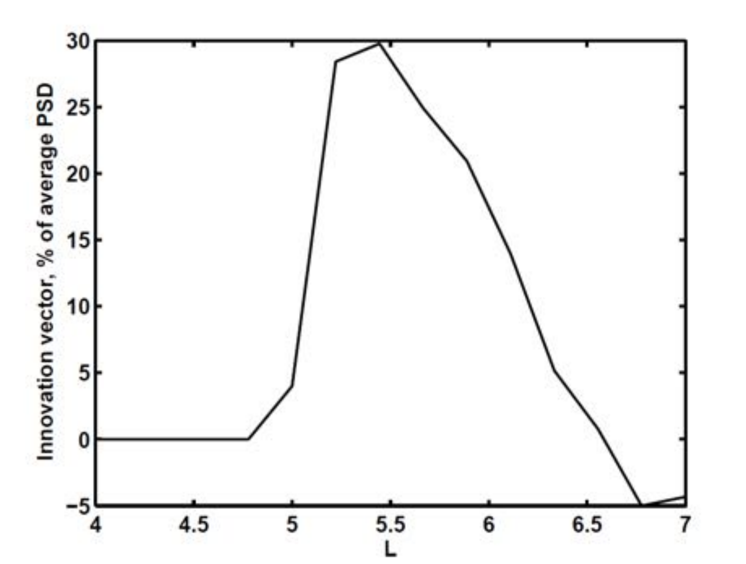

[Shprits et al., 2007]

$$X_a = X_f + K_t(y_t - X_f)$$

2D Data Assimilation

$$X_t^f = M_{t-1} X_{t-1}^f$$

$$X_t^f = M_{t-1\alpha} M_{t-1E} X_{t-1}^f$$